



Fort Lewis College SpaceHawks



HASP 2021 Final Report

Written by:
Nikolas Conmy, Hannah Carlson, Jessie Urban, Daniel Sandner, Humberto Arredondo Perez,
Roxie Sandoval, and Dr. Charles Hakes

Fort Lewis College
1000 Rim Dr.
Durango, CO 81301
December 2021
Revision 20211216a

Table of Contents

Abstract	5
1.0 Mission Overview	5
2.0 Design	6
2.1. Structure	6
2.2. Geiger Counters	11
2.3. Mobius Camera	14
2.4. Power Management System (PMS)	16
2.5. Thermal Management System (TMS)	19
2.6. COMMS	20
2.7. GPS	21
3.0 Project Management	22
3.1. Student Team	22
3.2. Project Timeline	22
3.3. Mass Budget	23
3.4. Monetary Budget	24
4.0 Testing Plan	24
4.1. Functional	24
4.2. Structural	25
5.0 Flight Logistics (PSIP)	26
6.0 Results, Analysis, and Conclusion	29
6.1. Geiger Counters	29
6.2. Mobius Camera	33
6.3. Power System	35
6.4. GPS and 9DOF	42
7.0 Failure Summary	44
8.0 Conclusions	44
9.0 Message to Next Year	46

Table of Figures

Figure 1: Final CAD design of the HASP sled structure.....	7
Figure 2: Final CAD design of the HASP casing.....	8
Figure 3: Constructed outer case showing sled spacing.....	8
Figure 4: Proposed (above) and final sled designs (below).	9
Figure 5: The finished HASP payload goes through final testing before integration.	10
Figure 6: Final design of the payload structure with some students' signatures.....	11
Figure 7: The SEN-10742 Geiger counter.....	12
Figure 8: Type 5 Geiger that used solid state technology from SparkFun [1].	12
Figure 9: Brass housing with servo exposing the lower two Geiger counters	13
Figure 10: Complete Geiger System in brass housing.	14
Figure 11: The Mobius Action Camera.....	15
Figure 12: Viewing hole in the outer case for the mobius camera.	15
Figure 13: The mounted mobius camera with power supply next to it.....	16
Figure 14: Power management system block diagram.....	17
Figure 15: Internal block diagram of the PMS.....	18
Figure 16: Front view of PMS 3D printed housing.....	18
Figure 17: Top view of PMS 3D printed housing.....	19
Figure 18: Temperature Sensors pin-out.....	19
Figure 19: Temperature Management System (TMS) monitors and maintains all subsystems' temperatures.	20
Figure 20: Simple I2C network example [6].....	21
Figure 21: Altus Metrum TeleGPS.....	21
Figure 22: Gantt chart for the HASP schedule for 2021.	23
Figure 23: NASA HASP structure with all payloads experiments of other universities getting ready to go into the chamber for thermal test.	26
Figure 24: Counts versus Altitude facing up.....	30
Figure 25: Counts versus Altitude facing down.....	31
Figure 26: Radiation versus Sun Angle facing up.....	32
Figure 27: Radiation versus Sun Angle facing down.,.....	32
Figure 28: View of the balloon from the mobius camera.....	33
Figure 29: Temperature Sensors within the payload versus time from power on.....	34
Figure 30: The Temperature sensors above and below the payload.....	34
Figure 31: Altitude vs Temperature	35
Figure 32: Comparison of SD PMS current data to the downlink telemetry PMS current data ...	36
Figure 33: Comparison of SD COMMS current data to the downlink telemetry COMMS current data.....	37
Figure 34: Comparison of SD TMS current data to downlink telemetry TMS current data.....	37
Figure 35: Comparison of SD Geiger's current data to the downlink telemetry current data.....	38

Figure 36: Comparison of SD current data for the GPS and altimeter to the downlink telemetry current data.....	39
Figure 37: Comparison of SD current data for the Mobius camera to the downlink telemetry current data.....	40
Figure 38: Close up view at the beginning of flight, of current draw from Geiger Counters and the servo.	40
Figure 39: Close up view of the Mobius Camera current draw before the flight.....	41
Figure 40: The COMMS current draw at the end of flight, demonstrating increases in current...41	
Figure 41: Payload Altitude over Time from Altus Metrum TeleGPS	42
Figure 42: Sun Angle from Vertical vs. Time	43
Figure 43: Azimuth Angle of Payload Orientation versus Time.....	43
Figure 45: Poster presentation at the Fort Lewis College Physics & Engineering Fall Welcome	45
Figure 44: FLC HASP Team poster at Physics & Engineering Fall Welcome Event	45
Figure 46: Team photo at Columbia Scientific Balloon Facility	46

Abstract

The Fort Lewis College's High Altitude Student Platform (HASP) team built an ionizing radiation measuring experiment RAT (Radiation vs Altitude and Time) as a cost-effective alternative to measuring high-energy radiation present in the atmosphere over changes in altitude and with respect to the sun angle. This payload was launched on a weather balloon platform from the Fort Sumner NASA balloon facility. The primary experiment uses two counter-facing Geiger-Muller-tube counters, and two counter-facing solid state detectors to record high-energy radiation. An accelerometer, barometer, and GPS were used to determine the altitude, orientation, and time of day. This is used to determine the sun's incident angle. The system was controlled by an Arduino Pro Mini with downlink data utilizing the HASP system as well as being backed up to a micro-SD card. A communication system (COMMS) was used to downlink the data. A power management system (PMS) monitored the power to each system using DC current sensors. A temperature management system (TMS) recorded the temperature of each system and activate heaters, as needed, to help maintain normal functionality. A digital camera system was installed on the payload to record flight events. Because of a hardware malfunction the RAT was unable to differentiate gamma from beta and alpha ionizing radiation. The upward and downward radiation as a function of altitude measured during the ascent are presented. The upward and downward radiation as a function of incident sun angle during the float are presented. A significant increase in radiation was detected on both the up-facing Geiger-Muller and solid-state detectors when the sun was less than 40 degrees from vertical. The payload lost power towards the end of the flight and the cause was unable to be identified.

1.0 Mission Overview

Fort Lewis College team built the radiation vs. altitude and time (RAT) payload that flew on the NASA/LSU High Altitude Student Platform (HASP). The primary goal of this experiment is to measure upper-atmospheric, ionizing Radiation vs. Altitude and Time (RAT). Time was recorded using the Arduino's internal clock, location from the HASP GPS, and orientation was recorded using the accelerometer and magnetometer in a Nine-Degree-of-Freedom (9DOF) stick. This is used to determine the location of the sun in relation to the payload. Radiation data was collected using two counter facing Geiger counters and two solid state radiation detectors. The Geiger counters used brass shutters that alternated between open and closed to differentiate between gamma and beta, or other ionizing radiation. Door control was done using a servo which alternated the shutters from covering and uncovering the detectors. When covered, gamma rays are the only ionizing radiation detected. When open, beta radiation can be detected as well.

The payload was also equipped with a temperature management system (TMS), power management system (PMS), and communication system (COMMS). The secondary goal was to incorporate a GPS and camera system. The GPS was implemented for easier access than the NASA GPS. The GPS system provides a reference for future payloads. The camera recorded the flight from liftoff to capture data on the sun's location in relation to the payload location. A

lithium battery was used to keep the camera clock working until the payload receives HASP power. The camera then utilized HASP power to operate.

The TMS recorded the temperatures of outside top, Geiger's, camera, COMMS, PMS, then outside bottom of the payload to be able to cross reference them with the data from the other systems if an anomaly occurred. The TMS provided heat to the systems monitored if the temperature dropped below -20°C , to maintain functionality. The COMMS system backed up the data from each system on a micro-SD card and control the downlink and uplink capability. Each system operates using Arduino Pro Minis through I2C. The previous versions of the systems mentioned above have been used by past Fort Lewis Collage teams for payload flights on HASP and weather balloon flights as part of the Colorado Space Grant Consortium Demosat balloon program.

2.0 Design

The payload design was composed of subsystems that each controlled a unique function. The payload design was split into sections. The first was the structure of the payload which included the materials, shape and the overall structure that kept all the other subsystems in place. This also included cable management and the surrounding shell box. The Geiger counters system detected ionizing radiation and recorded as counts per 30 seconds to a micro-SD card using an Arduino Module. Mobius camara system was used to keep physical tracking of the orientation of the sun and the balloon rupture. The PMS distributed power to each subsystem from the HASP main power source from commands. The power sent to each subsystem was recorded in a micro-SD card using an Arduino Pro mini. The TMS monitored the temperature of each of the subsystems and applied heat as needed. The TMS also saved all temperature data to an SD card using an Arduino module. COMMS received data from all subsystems, processed the data, and sent the data using downlink. This was achieved by sending commands to the COMMS to execute a task. The GPS system was an onboard transmitter that transmitted latitude, longitude, and altitude in real time.

2.1. Structure

The final payload structural design utilized two distinct parts, a sled, and an outer case. Both were composed of G10 fiberglass and secured to the provided mounting plate via two $\frac{1}{4}$ -20 threaded rods. The payload covered an area less that 6x6 inches and was 12 inches tall up to the top of the rods. The sled held all electrical components perpendicular to the mounting plate, as seen in Figure 1, and consisted of two 10x5x $\frac{1}{8}$ -inch-thick fiberglass sheets in which all the components were mounted. The colored boxes in the figure below represent the mounted components. The threaded rods passed through two separate aluminum spacers, placed between the sheets of the sled. The sheets were screwed to the spacers and nuts were used at the top and

bottom of the threaded rods to secure the sled in place. The outer case also held the sled vertically as the rods were permitted to protrude from the top.

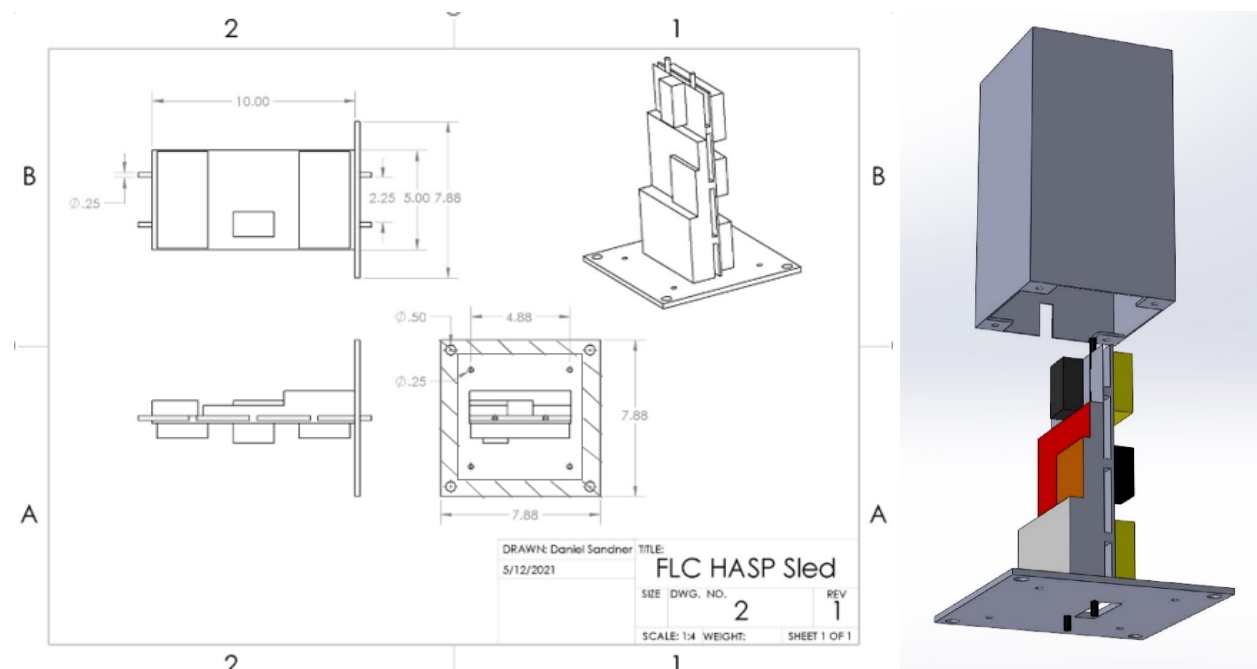


Figure 1: Final CAD design of the HASP sled structure.

The outer case was a rectangular case made of a thinner, 1/16-inch fiberglass and was held together with 1-inch L-brackets and bolts. The outer case used the threaded rods from the top of the sled and corner brackets on the bottom of the case to attach to the mounting plate. As the desired scientific goal was to detect solar radiation, a rectangular hole was made in the top of the outer case and the mounting sled to expose the Geiger Counters to direct radiation. Overall, the rectangular design maximized the payload's usable volume within the confines of the mounting plate dimension as shown in Figure 2 and Figure 3.

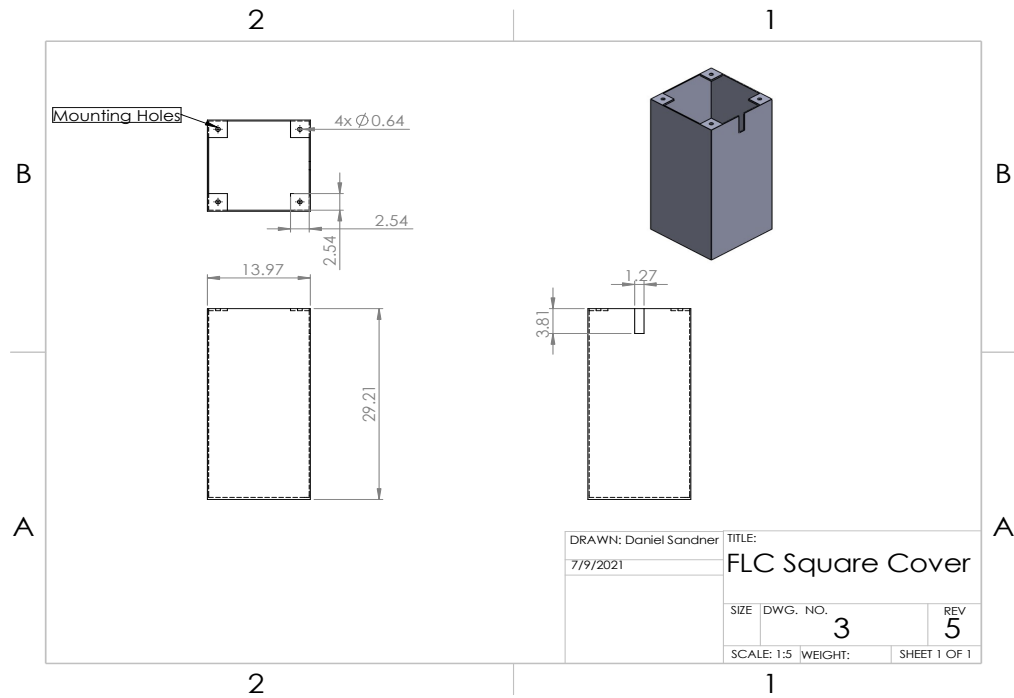


Figure 2: Final CAD design of the HASP casing.

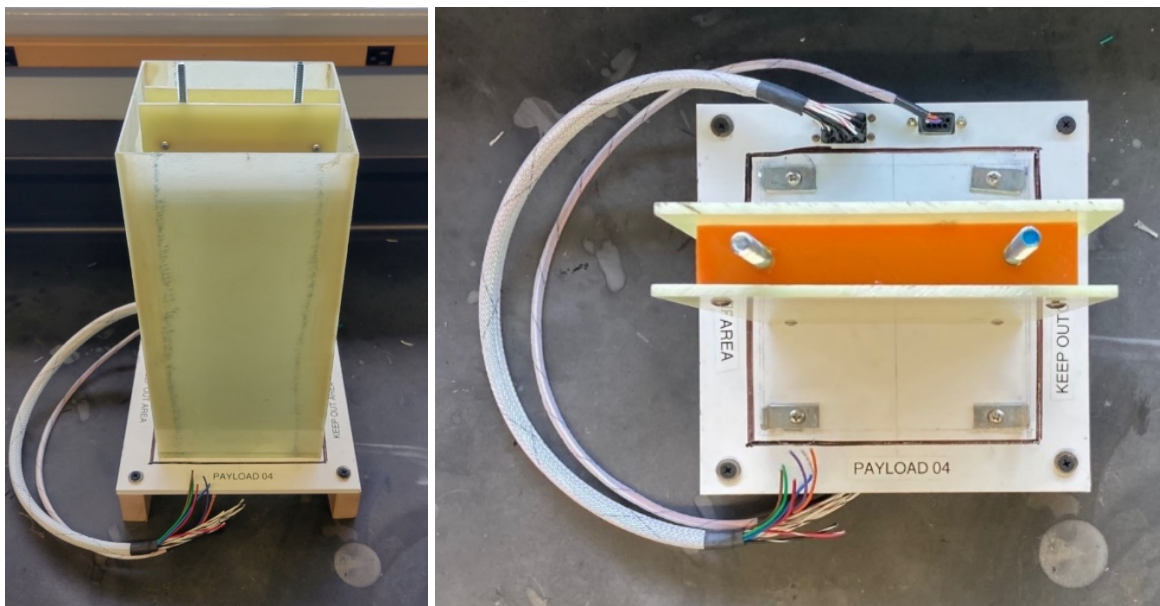


Figure 3: Constructed outer case showing sled spacing.

The electrical components were attached to both sides of the payload sled seen in Figure 3. The sled and case were designed to be slightly smaller than the maximum specified volume of 6x6x12 inches to accommodate any hardware that may protrude from the outer case. The internal layout stayed similar to the initial design. Side 1 of the sled held HASP systems while Side 2 held the Geiger Counter system.

Both finished sides of the final HASP design are shown in Figure 4. In the sled is shown mounted perpendicularly to the mounting plate with HASP systems on one side and Geiger systems on the other. Due to the square case, space was maximized, allowing for a push-rod door mechanism to open the Geiger counter enclosure. The final design was secure, strong, and easy to open for maintenance. All systems were adequately mounted and protected with this design.

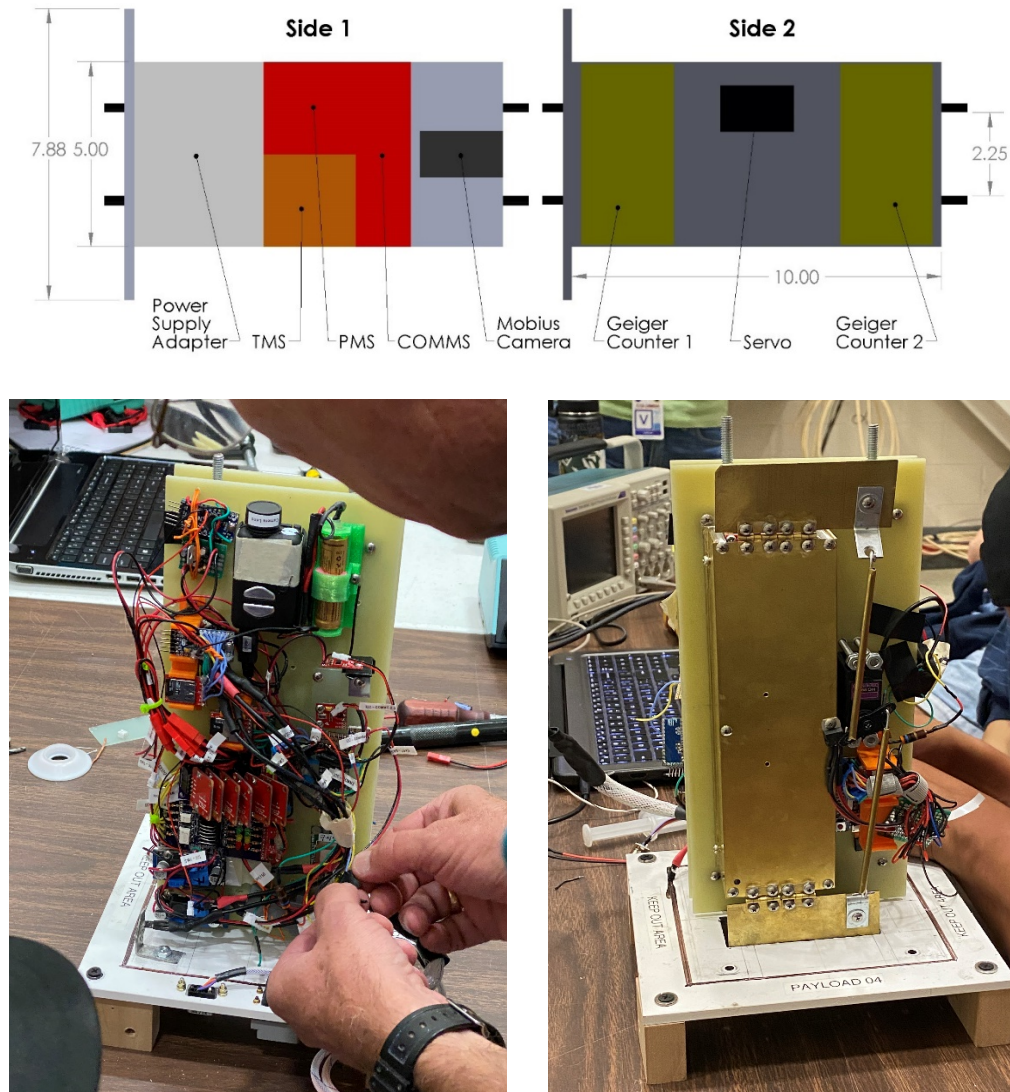


Figure 4: Proposed (above) and final sled designs (below).

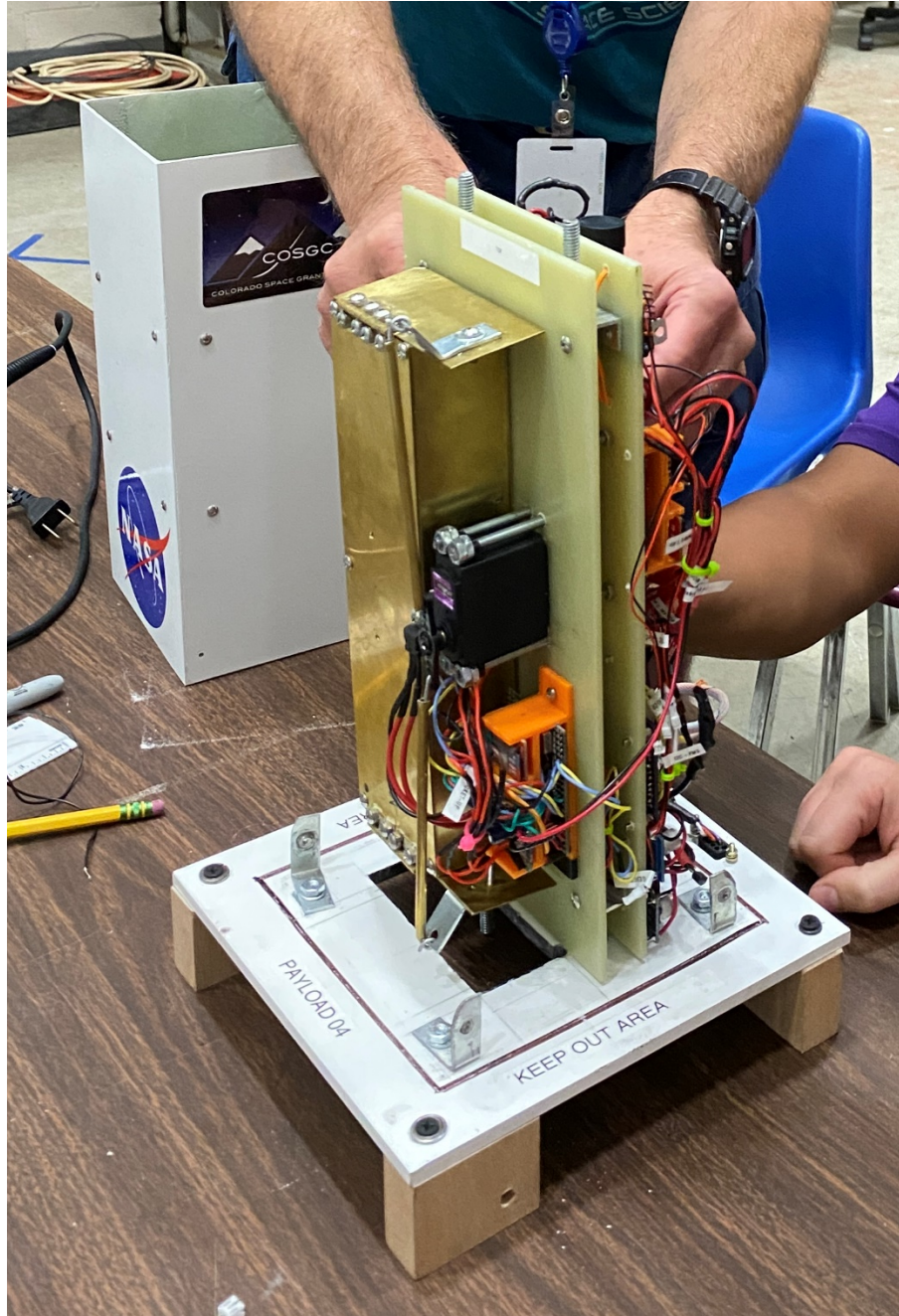


Figure 5: The finished HASP payload goes through final testing before integration.



Figure 6: Final design of the payload structure with some students' signatures.

The finished payload was painted in white, and some stickers were added to distinguish from other payloads (Figure 6).

2.2. Geiger Counters

Two different types of radiation detectors were used. The first radiation detector used a Geiger-Muller tube to detect ionizing radiation. The model used was a SparkFun Geiger counters seen in Figure 7.

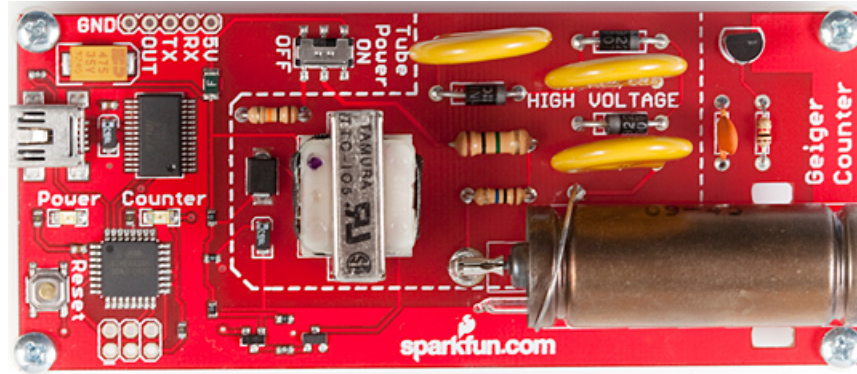


Figure 7: The SEN-10742 Geiger counter.

The tube in the Geiger contains inert gas and it has a window on the right side using the orientation of Figure 7. Particles enter through this window and interact with the atoms of the inert gas. The atoms release electrons and positively charged ions, the electrons move to the positive charged wire placed in the center of the tube and the ions move to a negatively charged tube wall. High voltage is used between the wire and the tube wall. This process creates an electrical pulse that travels through the wire and is read by a microcontroller that registers the pulse as a count. The SEN-10742 Geiger counter in particular triggers a buzzer and blinks a LED every time it gets an electrical pulse. The second type of radiation counter is the solid-state type 5 SparkFun sensor referred to as a Pocket Geiger (Figure 8). This Geiger is designed to detect ionizing radiation.

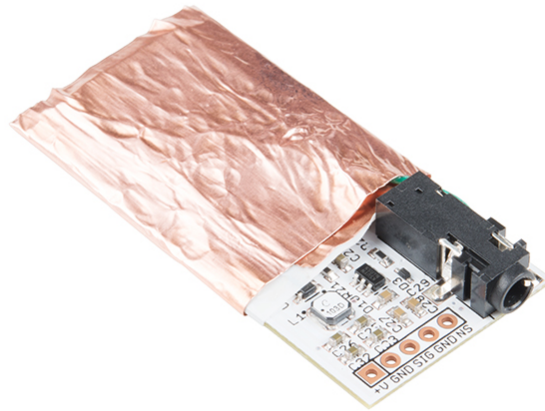


Figure 8: Type 5 Geiger that used solid state technology from SparkFun [1].

The solid-state radiation detectors create a signal from electrons that are removed from a semi-conductive material while ionizing radiation moves through it [5]. Ionizing radiation hits a front electrode and travels through a silicon medium and then hits the back electrode [5]. The back electrode becomes negatively charged and the front electrode (possibly more than one front electrode) becomes positively charged [5]. This is because the Geiger has a p-n junction that

creates an electric field that ionizes radiation that passes through it [4]. The current created is amplified and used to measure how much ionizing radiation is passing through the silicon at a certain instant. The pulse outputted can be read with any microcontroller.

The Geiger counters were placed in a brass case which blocks alpha and beta radiation. The Geiger Counters are configured so that one of each type are facing up and the other two are facing down. Their configuration is displayed Figure 10. The brass case has two gates that open and close every thirty seconds. A servo motor is utilized to open the gates on command. The purpose of the gates is to expose the Geiger counters to differentiate gamma radiation from alpha and beta (Figure 10).

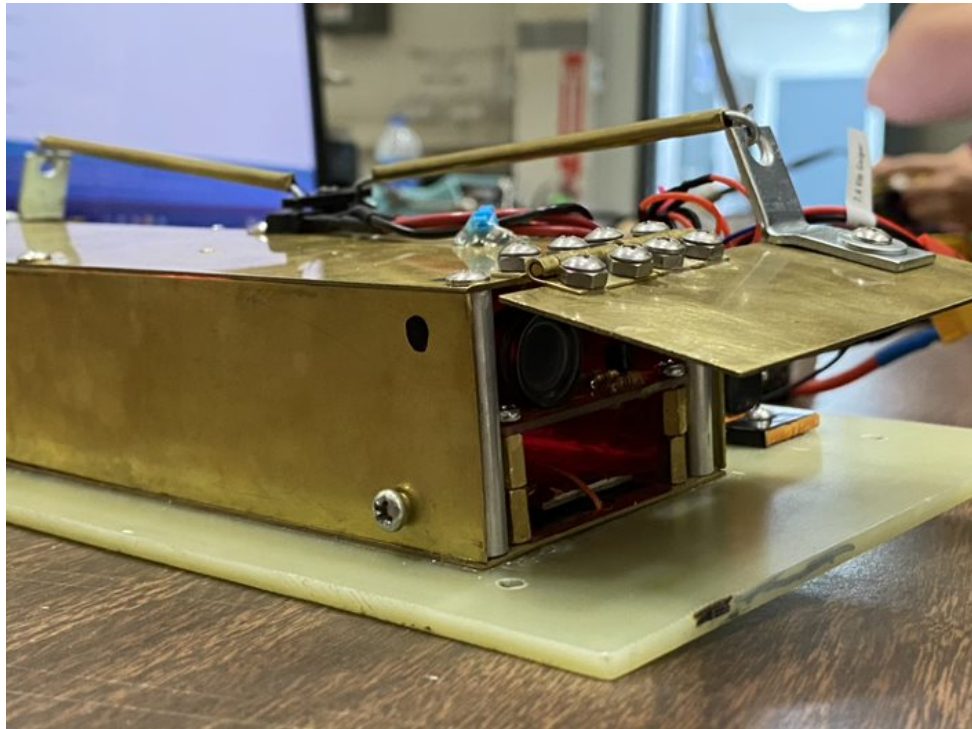


Figure 9: Brass housing with servo exposing the lower two Geiger counters

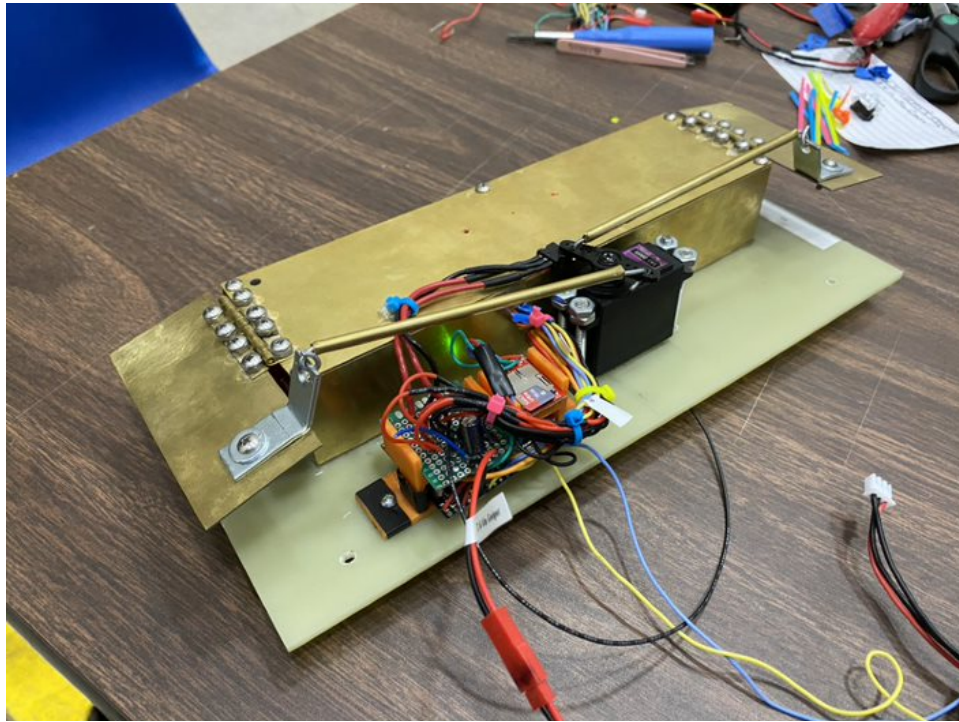


Figure 10: Complete Geiger System in brass housing.

The servos are controlled by an Arduino Nano. The case uses hinges and a rod to pivot the gates open. The Arduino Nano, SD card, and the prototype board are held by a 3D structure shown in Figure 10 (in orange).

2.3. Mobius Camera

The Mobius Action Camera is a small camera with programable features which the team has previously used aboard high-powered rockets and several other balloon flights (Figure 11). The camera is controlled by toggling the power provided to its USB port. Within the camera menu, certain power combos can control how the camera behaves. This feature is how our team controlled the camera during this and previous flights.



Figure 11: The Mobius Action Camera.

The mobius camera was mounted to Side 1 of the sled. The camera was attached at the top of the sled, peering through a small hole in the top of the outer case as shown in Figure 12. The goal of the camera was to catch the orientation of the sun and the moment the balloon ruptured.

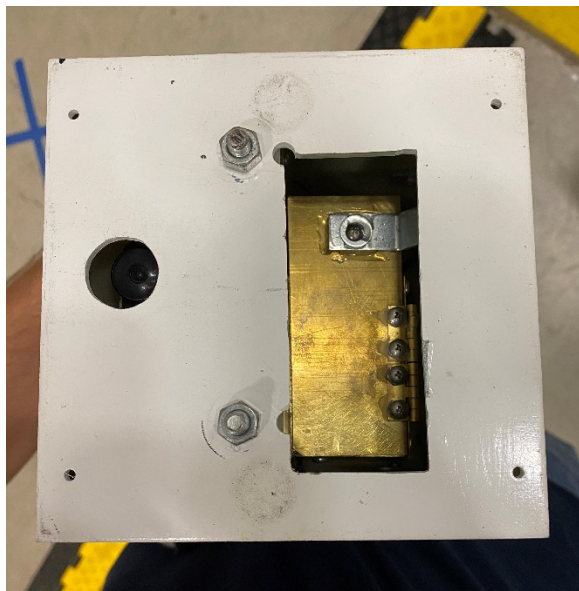


Figure 12: Viewing hole in the outer case for the mobius camera.

Using changes in power to control the camera via the PMS with commands sent through COMMS, the team was able to monitor current draw and toggle the camera. The camera was able to be powered on and off to either record steadily feed or enter toggle mode, where the camera would record ever minute for a few seconds to conserve SD card space. This means that it will record short videos in intervals that could be stitched into a time lapse. The camera received power from HASP only when the power was on for flight. However, when HASP power was disabled, the mobius camera could receive power from a payload battery to continue to operate in toggle mode as HASP returned to earth. Figure 13 shows the mobius camera in its mounted position.



Figure 13: The mounted mobius camera with power supply next to it.

2.4. Power Management System (PMS)

Figure 14 displays the power management system diagram. Power supplied by the HASP 20 EDAC connectors is wired directly to two LM3596 DC/DC converters. The supplied 30V is converted to 7.4V and 3.7V power using a DC-DC LM2596 converter which runs directly to the power management system (PMS). Each of the subsystem's currents are recorded by the PMS to and SD card and downlink (COMMS). The PMS provided the Mobius camera, Geiger counters, TMS, and COMMS with 7.4V. The altimeter, GPS, and 9DoF were supplied 3.7V from the PMS. Power provided by HASP will go to the PMS, which provided LED indication, and recorded using INA169 DC current sensors for the subsystems. The current data from each payload is recorded from the Arduino Pro Mini to a micro-SD every second.

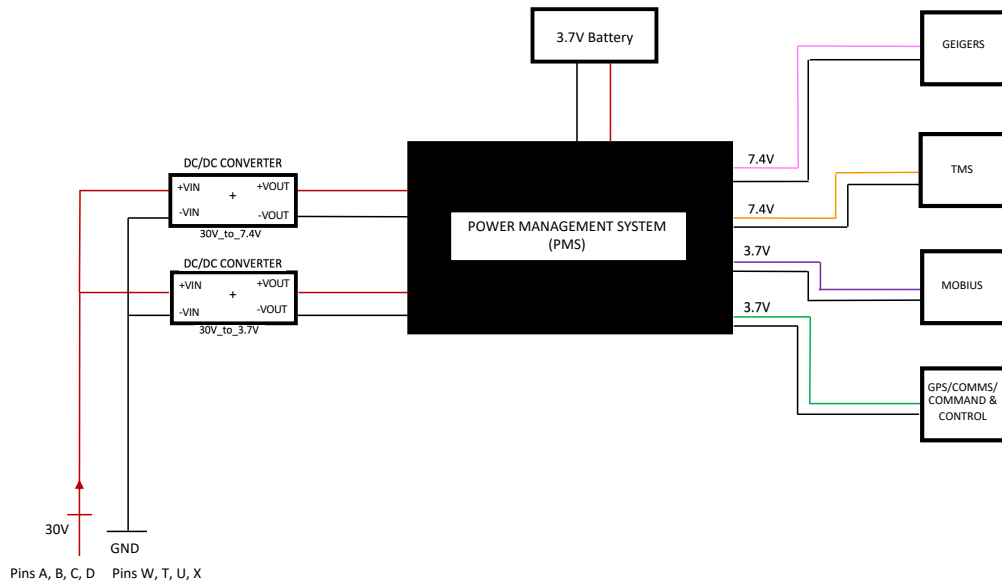


Figure 14: Power management system block diagram.

Table 1 below, demonstrates the subsystem’s voltages and their individual measured current draws. The LM2596 DC/DC converters have an effective efficiency of 92% when all systems are operating simultaneously. The effective draw is scaled by the entire payload draws an effective 442 mA from the 30V HASP power supply.

Table 1. Payload power usages.

Subsystem	Max Recorded Draw (mA)	Voltage (V)	Power Draw (mW)	Effective Draw @30V (mA):
Altus Metrum TeleGPS	190	3.7	703	28.9 ± 10
COMMS	40	7.4	296	10.9 ± 10
TMS	910	7.4	6734	21.7 ± 10
PMS	20	7.4	148	10.9 ± 10
Geiger Counters	150	7.4	1110	163.0 ± 10
Mobius Camera	330	7.4	2442	95.7 ± 10
DC-DC Conv.	10	30	300	10.9 ± 10
Buffer				100
Total:			11733	442 ± 26

Figure 14 displays the internal block diagram of the PMS. Power provided by HASP and the lithium-ion battery connects to an optical relay system. The optical relay system is controlled by an Arduino pro mini that allows the PMS to disable payload subsystems. All currents are measured by INA169 current sensors. The fuses are in line with the current

sensors to disable the payload if they receive too much current. All data is saved to a microSD card. The system illustrated in Figure 15 is repeated six times for each of the six different current sensors. Each current sensor range was calibrated by resistors.

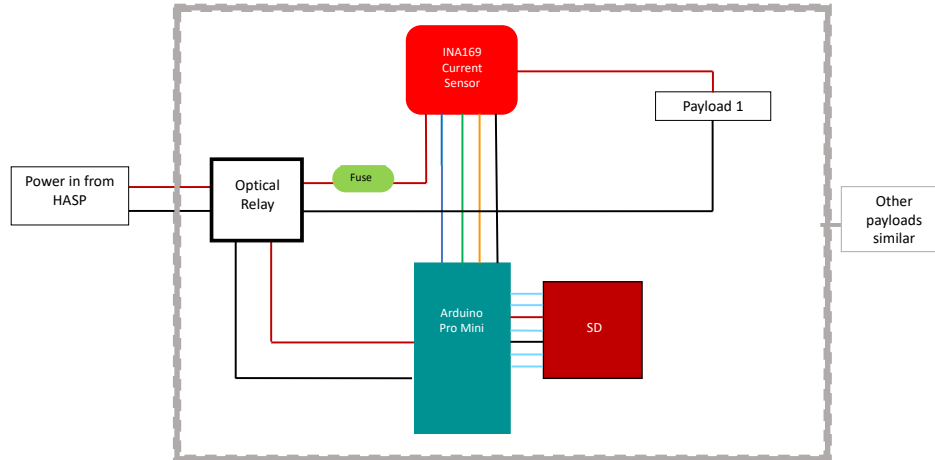


Figure 15: Internal block diagram of the PMS.

The Mobius camera uses a Tenergy 3.7V 800mAh, UL-listed Lithium-ion batteries to keep the timestamp on it only. This system could be used to as an internal power source for the payload but was only used to keep the time stamp on the camera. All subsystems have internal fuses that protect from current surges.

Figure 16 and Figure 17 show the PMS housing. The housing is a very simple design with two shelves. The bottom shelf has two slots for the SD card holder and the Arduino pro-mini. There are ridges in place for both electronics to slide in and remain secured throughout flight. The top shelf is designed to hold the PMS PCB. The housing was made with a 3D printer using ABS plastic.

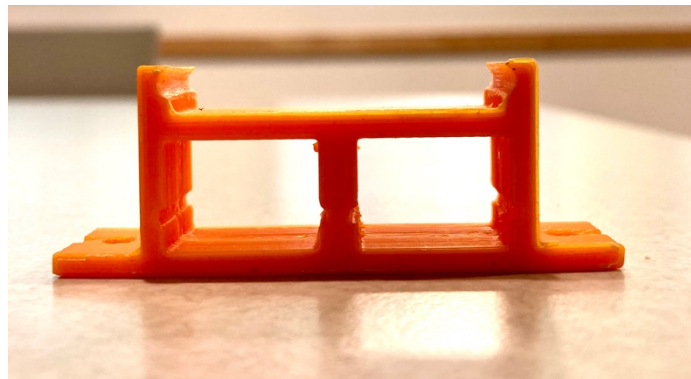


Figure 16: Front view of PMS 3D printed housing.

Figure 17 shows a top view of the PMS housing. The two holes on both sides of the base are in place for screws to attach the housing to the fiberglass sled.



Figure 17: Top view of PMS 3D printed housing.

2.5. Thermal Management System (TMS)

The temperature management system (TMS) monitors the temperature of each of the subsystems and if necessary, heat the systems. The TMS PCB, Arduino and SD card reader are all situated in a 3D printed housing where the PCB is on the bottom while the Arduino and SD reader are on top. The TMS also saves all temperature data to an SD card.



Figure 18: Temperature Sensors pin-out.

There were six temperature sensors (Figure 18) in essential positions throughout the payload. The sensors placement starting from the left where the red arrow is pointing in Figure 19 are the bottom outside of the payload, the PMS, the COMMS Arduino, the camera's battery, the servo for the brass doors, and the top of the outside of the payload.

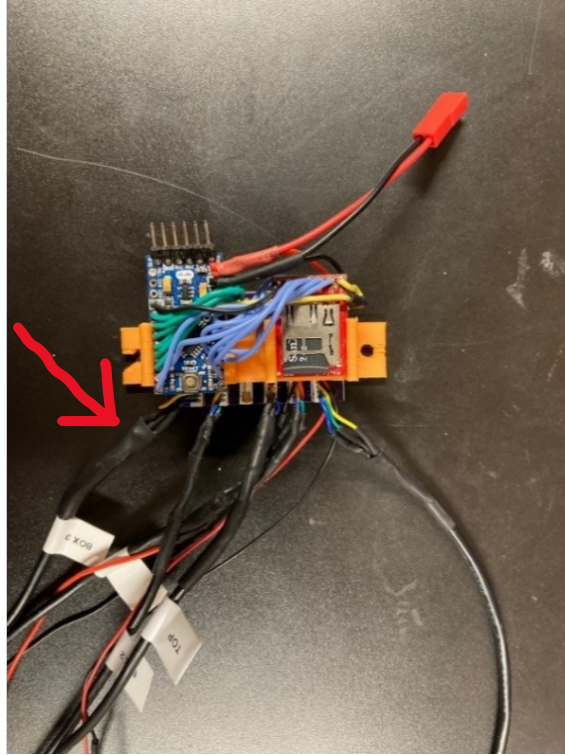


Figure 19: Temperature Management System (TMS) monitors and maintains all subsystems' temperatures.

2.6. COMMS

The communications system received data from all subsystems and processed it for downlink, additionally, it did interface with all other enabled subsystems to send uplinked commands. An Arduino microcontroller was used to coordinate uplink and downlink commanding. A 1200 baud rate and RS232 logic were used for the interface.

The data interface was initiated at the DB9 connector on the HASP platform. The data transmission lines were feed into an RS-232 to TTL converter, which allows an Arduino microprocessor to control the communications. These converted lines will then feed directly into the Arduino, which interfaces with each system in a separate I2C communications process. Figure 20 demonstrates a simple I2C connection with a master device and multiple slave devices.

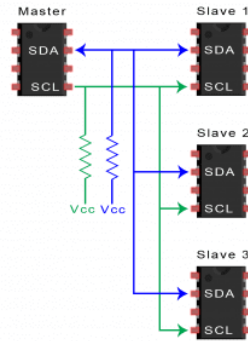


Figure 20: Simple I2C network example [6].

All downlink data will be packetized. The maximum downlink rate will be 544 bps. Strings will be no more than 64 bytes in length. They will be transmitted on a two second cycle.

The structure for the COMMS was simple. A fiberglass sled was cut for all the COMMS components to be attached. The COMMS sled was mounted onto the larger sled with ¼” 4-40 stand-offs. All components were attached to the smaller sled with 4-40 screws and secured with zip ties.

2.7. GPS

Figure 21 shows the Altus Metrum TeleGPS used on the payload. This flight computer, developed for use in tracking high-powered rockets, has an on-board transmitter for the 434.55 MHz band. Basic telemetry is transmitted and stored internally: latitude and longitude.



Figure 21: Altus Metrum TeleGPS

3.0 Project Management

3.1. Student Team

Table 2: Task Assignments

Task	Person(s) in charge
Management and Documentation	Hannah Carlson, Nikolas Conmy, and Dr. Charles Hakes
Geiger Counters	Humberto Arredondo Perez
Power System	Jessie Urban
Communications	Jessie Urban and Roxie Sandoval
Mobius Camera	Roxie Sandoval
Thermal System	Hannah Carlson
Structure	Daniel Sandner
Testing	ALL
Participants	Cheyenne Tucson and Mark Heltman

3.2. Project Timeline

We had many issues with time for our trouble shooting. Figure 22 shows our Gantt chart including the milestones.

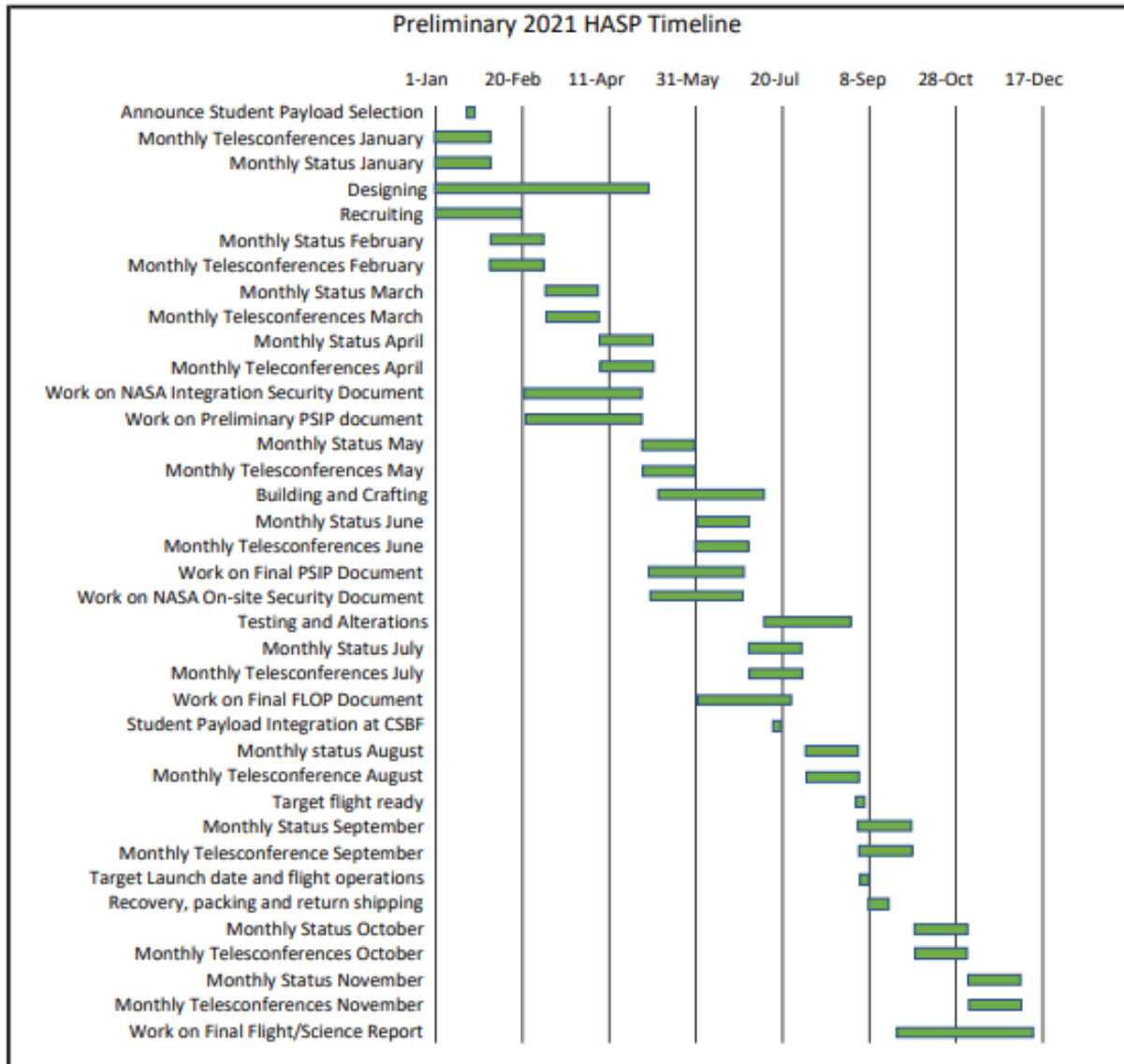


Figure 22: Gantt chart for the HASP schedule for 2021.

3.3. Mass Budget

Table 3: Weight of the subsystems

Subsystem	Weight (g)
Mobius Camera	61.7
Payload sled	500
Internal Structure pallet	39.6
GPS*	23.8
Fiberglass case	1000
Geiger counters	200*2
Total	2025

The weight of most of the systems came from the measurements of similar systems that flew on the 2020 Demosat balloon launch. The maximum weight for the small payload is 3kg and the size of the payload cannot exceed 15cm in width and 15cm in length.

3.4. Energy Budget

Table 4: Power use by the various sub-systems

Component	Power (watt)	Voltage (volts)	Current (amps)
PMS, COMMS, GPS	1.5	3.3	0.45
TMS	0.75	5.0	0.15
Mobius Camera	2.5	5.0	0.5
Geiger Counters	0.15	5.0	0.03
Total	4.9	18.3	1.13

The maximum power supplied from the HASP is 28 volts at 0.5 amps which equals 14 watts. The payload will use DC to DC converters to reduce the voltage and increase the current. This means that before this system a 0.5-amp fuse will be used to make sure the payload does not exceed the 0.5-amp limit.

4.0 Testing Plan

4.1. Functional

Each sub-system was initially tested to determine if they were functional. The Subsystems include the Geiger counters, COMMS, TMS, PMS, Mobius Camera, and GPS. The COMMS TMS, COMMS, and Geiger counters had their own micro controllers that were tested through the Arduino app to see if the data recorded was accurate. The systems were then wired with power from the PMS and I2C connections to the COMMS. The COMMS was tested to verify that downlink communication was recording the data in a computer display port. To determine if each system was receiving and responding to commands, we tested the uplink commands by using a display port to determine the sub-system's response. Micro SD cards were used for local storage for the TMS, PMS, Geiger counters, and Mobius camera. Each SD card reader was checked after testing the system to see if the expected data was being recorded. A full system test was done to determine if everything ran as expected. The system test included checking if the TMS provided heat to systems when a temperature of -20°C was reached.

During Integration the payload was tested in the following manner. The payload was mounted to the HASP platform and attached to the electrical and data connections. All subsystems (Geiger Counters, GPS, MoCam, PMS, TMS, and COMMS) began functioning as designed upon first power cycle. The COMMS system downlinks appropriate data and receives uplinked commands. The Mobius camera, TMS, Geiger Counters, and GPS can be disabled and enabled

by serial command. All systems and components remain securely attached to the structure and functioning as designed throughout thermal / vacuum testing.

The steps for integration are the following:

- Initialize microSD cards and install them to proper subsystems.
- Secure subsystems on sled, insert sled into housing and align each subsystem.
- Mount payload to the HASP platform/Close power supply circuit.
- Check for serial downlink/analyze for proper power activity/LED indicator display.
- Send all commands through uplink to verify uplink.
- Analyze LED indicator display for successful command execution.
- Unmount payload/access payload data (subsystem microSD cards).
- Analyze integrity of recorded payload data for all systems.
- Check Mobius data to ensure camera records in correct time intervals.

4.2. Structural

A thermal and vacuum test were conducted on July 30th. The payload was attached to the HASP platform and placed inside a vacuum chamber for approximately six hours. After the vacuum chamber test, the housing for the payload was analyzed for any structural damage. No damage was found. The Payload structure held up under a vacuum test and a thermal test from -50°C to 50°C . A hang test and drop test were considered unnecessary due to the configuration of the payload attachment to the HASP platform. The payload used threaded $\frac{1}{4}$ -20 rods to hold the structure together and it's been used in previous experiments successfully. The payload can be seen in Figure 23, ready to go into the chamber for testing.



Figure 23: NASA HASP structure with all payloads experiments of other universities getting ready to go into the chamber for thermal test.

5.0 Flight Logistics (PSIP)

A. Date and Time of your arrival for integration:

We plan to arrive on the first day of integration on July 26th at 9 am.

B. Approximate amount of time required for integration:

We approximate 5 hours of payload time outside the thermal / vacuum test chamber are needed for a full systems checkout; this includes testing the commands which can be seen in the table of part D, section IV, mentioned above. After this checkout, we estimate that approximately 15 minutes will be required for the pre-integration checks (5 minutes for mechanical checks, and 10 minutes for power and uplink/downlink checks).

For proper integration, we estimate that 45 min will be required as detailed:

1. 10 minutes for mechanical/electrical connection to the platform
2. 20 minutes to verify proper payload operation:
 - a. 5 minutes to close power supply circuit / verify payload ON.
 - b. 5 minutes to analyze downlink / verify appropriate critical subsystem function.

- c. 10 minutes to cycle all uplink commands / verify appropriate behavior.
3. 15 minutes for administrative functions.
- C. Name of the integration team leader: Hannah Carlson
- D. Email address of the integration team leader: hgcarlson@fortlewis.edu
- E. List **ALL** integration participants (first and last names) who will be present for integration with their email addresses:

Participants:	Contact Information:
Hannah Carlson	Hgcarlson@fortlewis.edu
Jessie Urban	Jpurban@fortlewis.edu
Nikolas Conmy	Ngconmy@fortlewis.edu
Daniel Sandner	Dssandner@fortlewis.edu
Cheyenne Tucson	crtucson@fortlewis.edu
Humberto Arredondo	Harredondoperez@fortlewis.edu
Roxie Sandoval	rlsandoval@fortlewis.edu
Charles Hakes	Hakes_c@fortlewis.edu

- F. Define a successful integration of your payload:
- i. The payload has no difficulty mounting to the HASP platform or provided electrical and data connections.
 - ii. All subsystems (Geiger Counters, GPS, MoCam, PMS, TMS, and Comms) begin functioning as designed upon first power cycle.
 - iii. The Comms system downlinks appropriate data and receives uplinked commands.
 - iv. The Mobius camera, TMS, Geiger, and GPS can be disabled and enabled by serial command.
 - v. All systems and components remain securely attached to the structure and functioning as designed throughout thermal / vacuum testing.
- G. List all expected integration steps:
- i. Initialize microSD cards and install them to proper subsystems.
 - ii. Secure subsystems on sled, insert sled into housing and align each subsystem.
 - iii. Mount payload to HASP platform/Close power supply circuit.

- iv. Check for Comms serial downlink/analyze for proper power activity/LED Indicator display.
 - v. Send all commands through uplink to verify uplink. Analyze LED Indicator display for successful command execution.
 - vi. Unmount payload/access payload data (subsystem microSD cards).
 - vii. Analyze integrity of recorded payload data for all systems.
 - viii. Check Mobius data to ensure camera records in correct time intervals.
- H. List all checks that will determine a successful integration:
- 1. Geiger Counters
 - a. Initializes reliably during HASP Integration without requiring any intervention.
 - b. Begins recording the high energy Gamma and Beta rays at proper recording intervals.
 - 2. Mobius Camera
 - a. Initializes reliably during HASP Integration without requiring any intervention.
 - b. Begins recording useable video feed after initialization at proper recording intervals.
 - 3. TMS
 - a. Initializes reliably during HASP Integration without requiring any intervention.
 - b. Begins recording accurate system temperature data after initialization, standing by to heat as necessary.
 - 4. PMS
 - a. Initializes reliably during HASP Integration without requiring any intervention.
 - b. Begins monitoring all subsystem power usage data when HASP power supply circuit is closed.
 - 5. Comms

- a. Initializes reliably during HASP Integration without requiring any intervention.
- b. Successfully establishes serial communication, including initializing data downlink and demonstrating successful command uplink.

6. GPS

- a. Initializes reliably during HASP Integration without requiring any intervention.
- b. Begins recording position data as designed after initialization, even if GPS signal is not immediately acquirable inside the integration facility.

I. List any additional LSU personnel support needed for a successful integration other than directly related to the HASP integration (i.e. lifting, moving equipment, hotel information/arrangements, any special delivery needs...):

None

J. List any LSU supplied equipment that may be needed for a successful integration:

None

K. COVID precautions

The Fort Lewis Space Hawks will all be fully vaccinated by integration week. We are following CDC guidelines while working together and any additional Columbia Scientific Balloon Facility requirements.

6.0 Results, Analysis, and Conclusion

The payload data results were recorded individually. The Geiger counters, the Mobius camera, The PMS system, The TMS system, the COMMS system, and the GPS system are explained in detail below.

6.1. Geiger Counters

Data was recorded from four different Geiger counters onto an internal micro-SD card. The telemetry from the Geiger system was unreliable and not used. One pair of detectors was facing up and one pair was facing down. The doors of the Geiger's housing were jammed at some point during the flight so, the difference between open and closed door is not clear. The relationship between counts, altitude and sun angle are shown below where, where G-M is for Geiger-Muller, Pocket is for the solid-state Type 5, Up is for orientation, 0 is for door closed, and 1 is for door open. In Figure 24, all data show a minimum number of counts when the payload was close to

the Earth's surface. As the altitude increased, the Pocket registered an increment on counts, but the G-M registered a minimum count. After about 60000 ft, the counts started to get fewer for the Pocket, and it dropped to almost none once the payload reached the stability in the flight at the maximum altitude. The data suggested that the Pocket must have a higher sensitivity compared to the G-M to certain radiation found at mid-altitudes. Just as it was mentioned before, the difference between open-door and closed-door counts is not distinguishable.

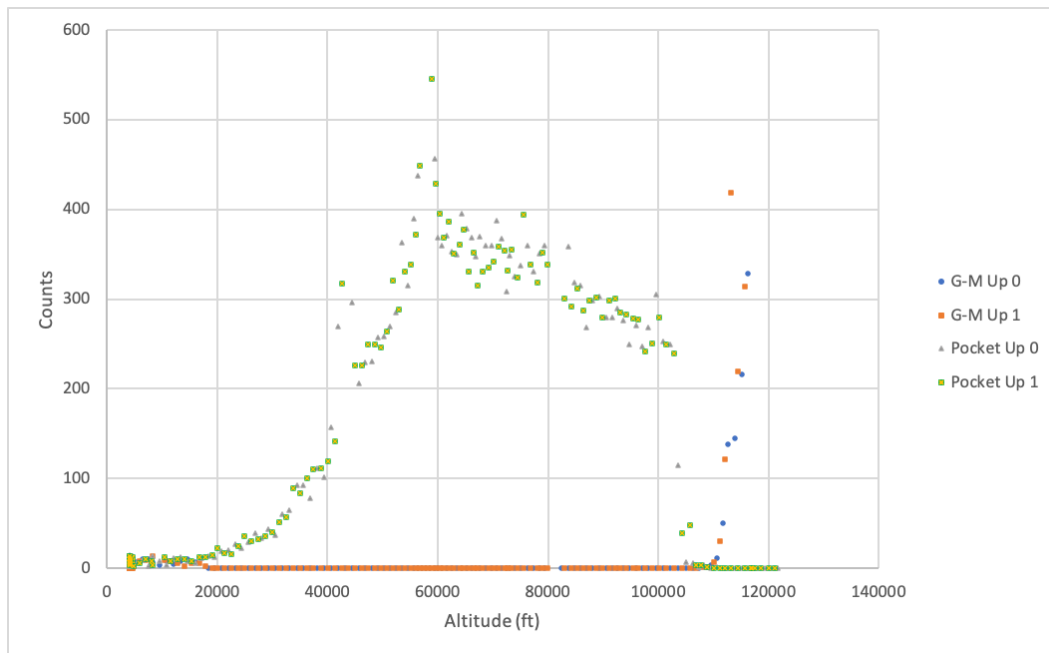


Figure 24: Counts versus Altitude facing up.

In Figure 25, the data for the down-facing detectors shows a similar count to the ones facing up when the payload was closed to the surface. As the altitude increased, the Pocket registered an increase in counts. The G-M registered a higher count compared to the ones facing up but not as many as the Pocket. The maximum counts were recorded about 70000 ft by the Pocket. The counts by the G-M counts were slightly higher than the ones facing up. According to the Pocket results, the difference between Up and Down is not noticeable enough to say they are different. When the payload was closed to the ground, the counts were almost none. The reason for this is believed that the radiation gets absorbed by the atmosphere and the scatter of particles is minimum. Halfway going up in the atmosphere, radiation tends to get scattered by the atmosphere and therefore, the Geigers are able to register this change.

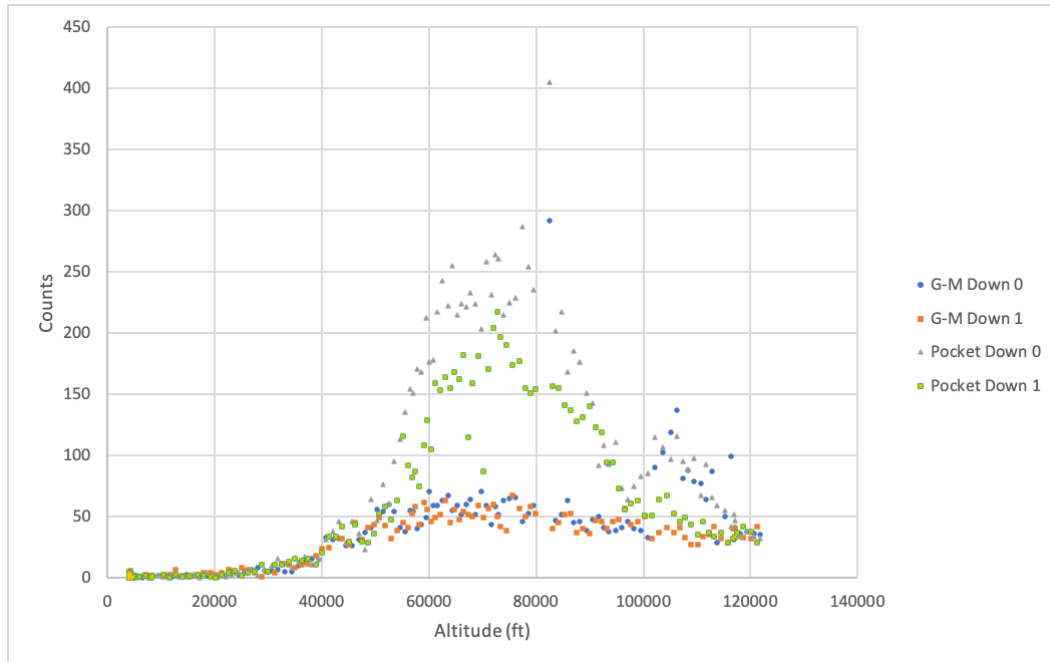


Figure 25: Counts versus Altitude facing down.

In Figure 26, the relationship between radiation counts of Geigers facing up and the angle of the sun is shown. The data used for this plot is from when the payload was stable at constant altitude. The angle of the sun was measured from the vertical, so an angle of zero represents the sun being right above the payload. The counts registered with a small angle were getting more counts which suggest that the sun was able to directly face the Geigers. The range of the counts at this point suggested that the payload was at moments under the shade of the balloon was a possibility. As the angle was greater, the counts reduced until almost none, which suggests that this radiation was being block by the Geiger's housing.

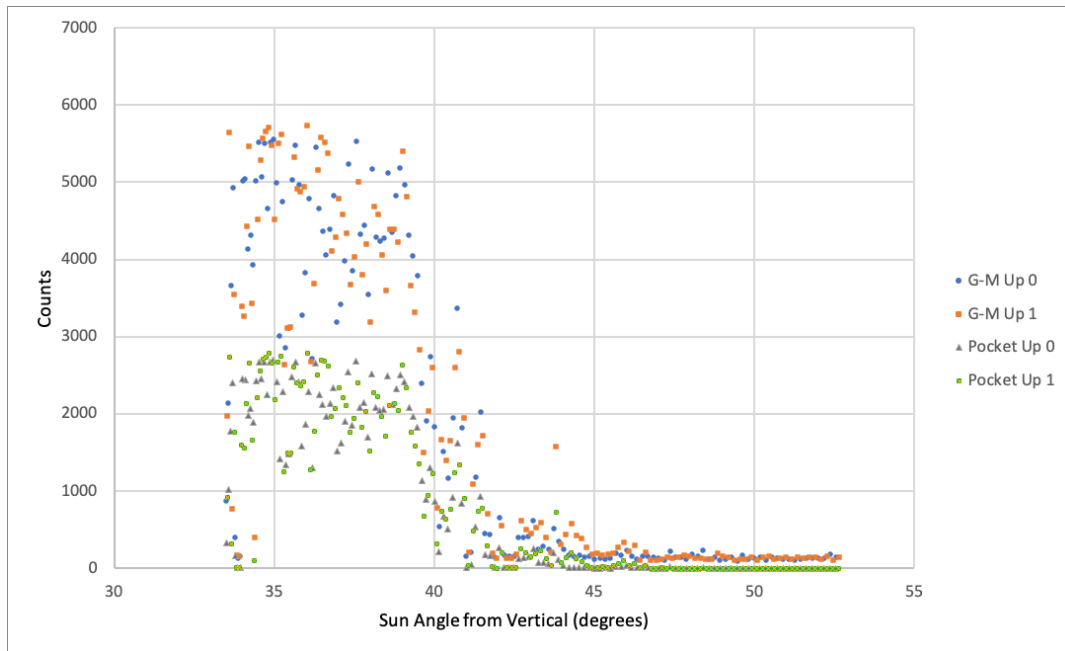


Figure 26: Radiation versus Sun Angle facing up.

Figure 27 shows the relationship between counts and the angle of the sun with the Geigers facing down. The data shows no change between counts and the position of the sun. Since the Geigers were facing down away from the direct light from the sun, it was believed that this is the reason of this result.

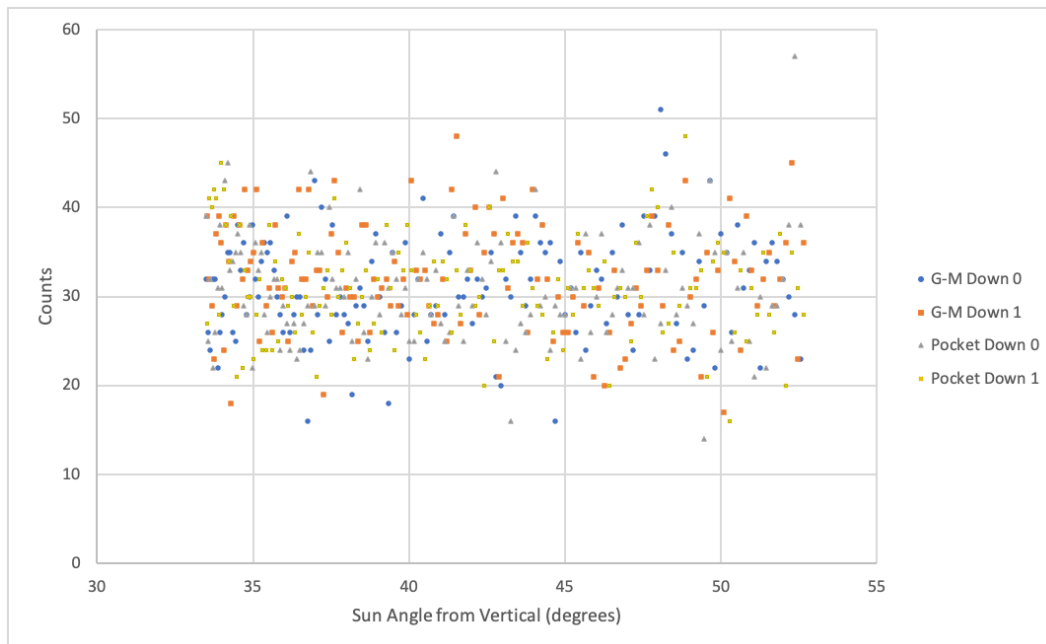


Figure 27: Radiation versus Sun Angle facing down.,

6.2. Mobius Camera

The mobius camera capturing the balloon burst was not successful. The camera was toggled on periodically but only a few of the files recorded were saved. Additionally, the camera battery was bad and did not supply adequate power. This meant that any accurate time stamp on the various video files was lost. Figure 28 shows the view of the balloon from the camera's perspective taken from the little footage gathered. Although a unique view, the camera did not capture the rupture, this may have to do to an overheating issue the payload experienced. The team will plan a better camera alternative in future years to capture inflation sequence and balloon rupture.

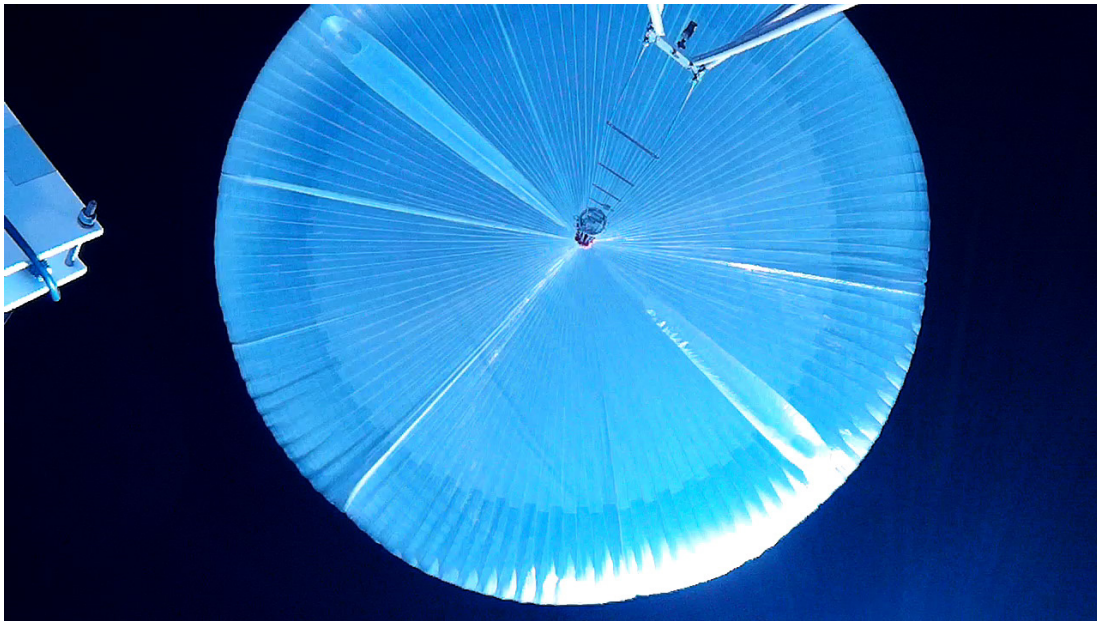


Figure 28: View of the balloon from the mobius camera.

6.3 Temperature Management System (TMS)

Our temperature sensors measured the temperature of each subsystem during the flight as seen in the graphs below. The temperature initially increased because the payload was taken outside of the warehouse and the morning ambient temperature was increasing. The temperature decreased rapidly as the altitude increased until the payload hit 60,000 ft. Then the temperature steadily increased throughout the flight. The graph ends early due to a power loss.

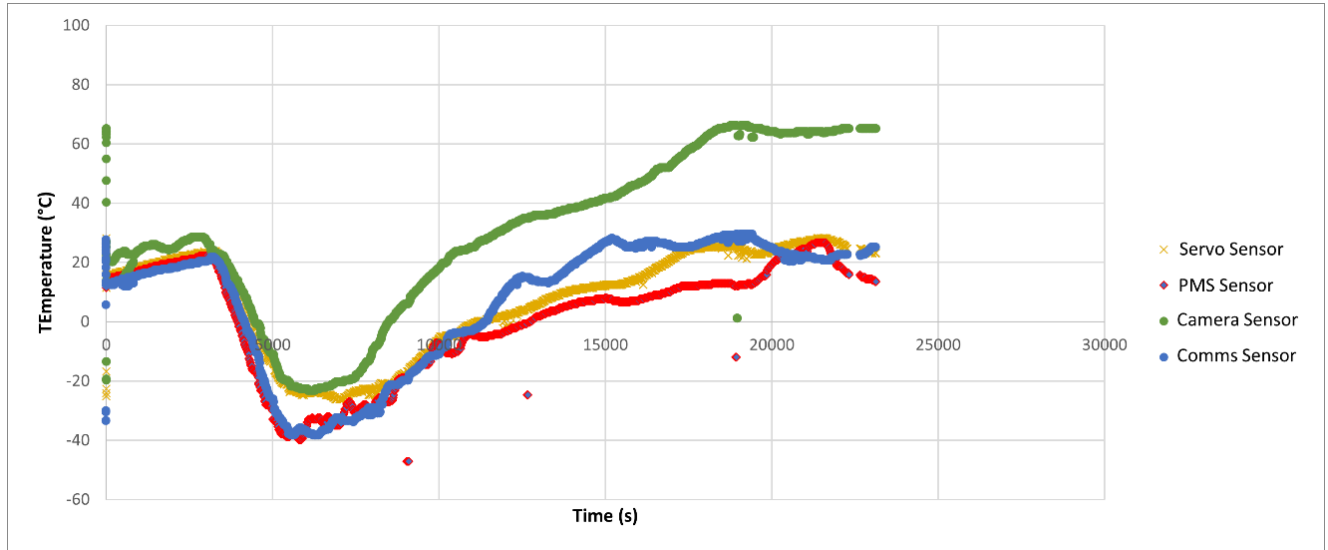


Figure 29: Temperature Sensors within the payload versus time from power on

In Figure 29, we see the temperature of the servo for the Geiger Counter’s brass doors as the yellow line. The temperature decreased past -20°C a little, so we believe that the heater placed next to the servo did turn on but did not reach its maximum temperature. The sensor for the camera is in green where we can see that the camera’s battery did not reach over -20°C . This shows that the heater placed by the battery worked as designed. However, the temperature of the PMS did go below -20°C as seen in red which tells us that the heater placed there was defective. The sensor for the COMMS can be seen in blue which also seemed to not function properly due to the temperature also exceeding below -20°C .

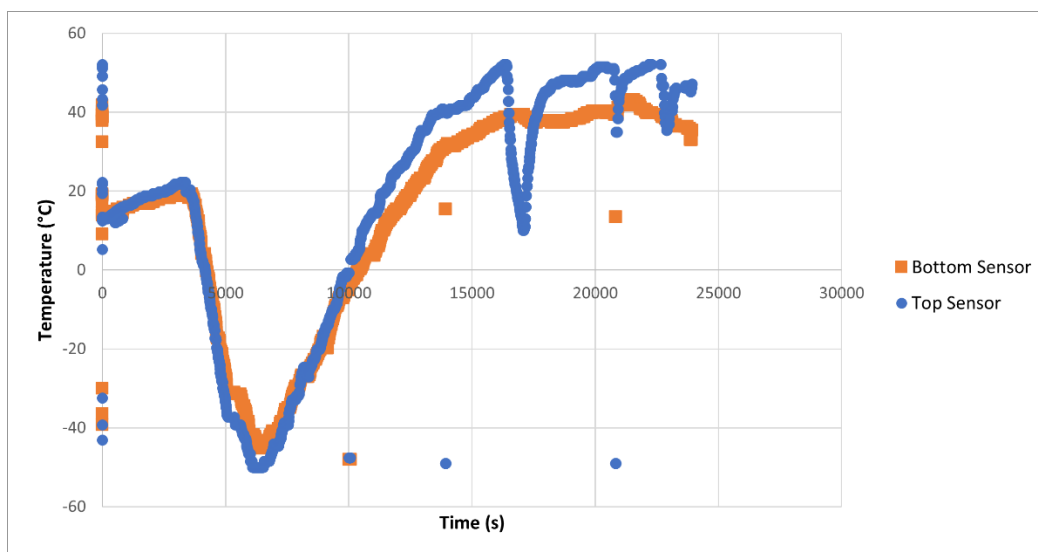


Figure 30: The Temperature sensors above and below the payload.

Seen above in Figure 30, the relationship between the two sensors that were outside of the payload are shown. The two sensors follow a similar path that describes the outside temperature, however, there are some spikes to a lower temperature from the sensor that was on top of the payload. These spikes suggest the payload was in a shadow for those moments and blocked from the sun.

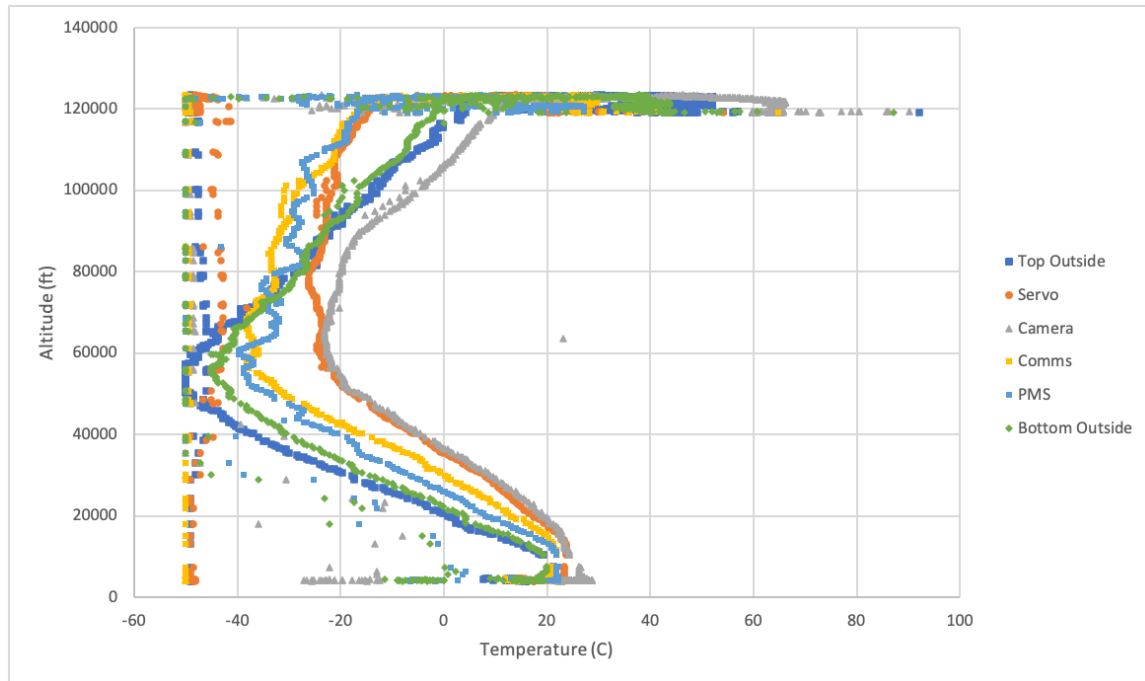


Figure 31: Altitude vs Temperature

Figure 31 shows the relationship between the altitude measured in feet and the temperatures of the payload subsystems. Each sensor reports about the same path. The relationship shows that the temperature decreased at mid-altitudes and then increased at higher altitudes, as expected. The temperatures recorded near -50 C were from RF interference, and later file formatting made those erroneous values more difficult to filter out.

6.3. Power System

Figures 32 through 37 demonstrate the difference in current data provided by the SD card and the telemetry data received during flight. For the following graphs the orange triangles represent the SD data, and the blue circles represent the telemetry downlink data. The SD data has more significant figures than the telemetry data causing the spread of the data to appear more spikey and jagged than the telemetry data spread.

Figure 32 displays the difference between the SD and telemetry recordings of current draw for the power management system. The telemetry current is much more spread out than the SD current. The larger spread in data could be attributed to the sampling rate of downlink. The time

interval in-between telemetry data collection is much larger than the time between the SD's data collection. The SD recorded data every second while downlink was only recorded every 15 seconds. The spread could also be caused by rounding in the telemetry data compared to the lack of rounding in the SD data, which is demonstrated by the number of significant figures in the SD data.

Current draw from the PMS stayed within a 0.01 to 0.04 amp range for the entire flight. Majority of the PMS current is clumped around .035 amps. After analyzing the data, there appears to be a few outliers along the 0.01 amp line. We expected a current draw of 0.01 to about 0.02 amps for the PMS, so the outliers are not unusual and well within the current range for the PMS.

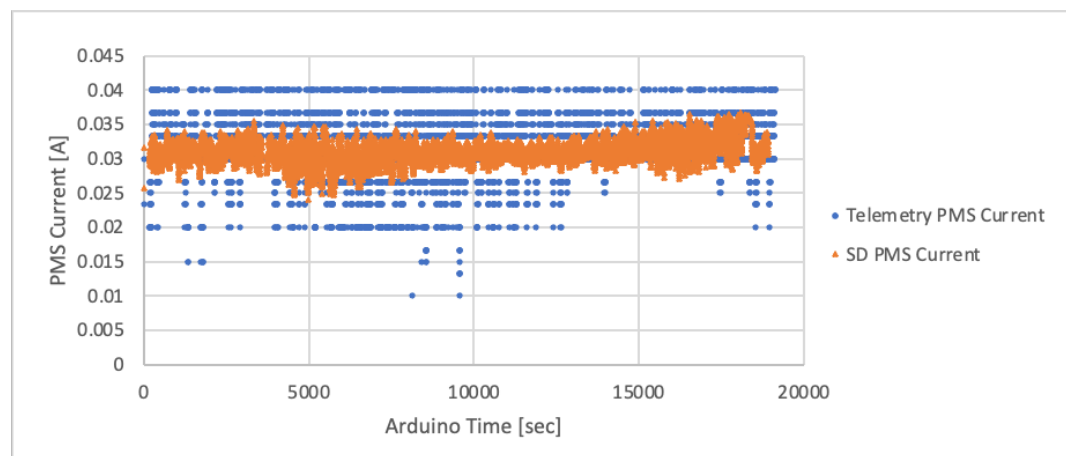


Figure 32: Comparison of SD PMS current data to the downlink telemetry PMS current data

COMMS pulled a range of 0 to 0.01 amps during the flight. This range is very similar to our expected amperage of 0.01. Figure 33 displays some outliers around 2000 seconds to 3500 seconds. After reviewing other data from the flight, we are still unsure of what caused these outliers. Even though the data set does include some outliers, the amperage the outliers reach is still minimal and plausible for the COMMS.

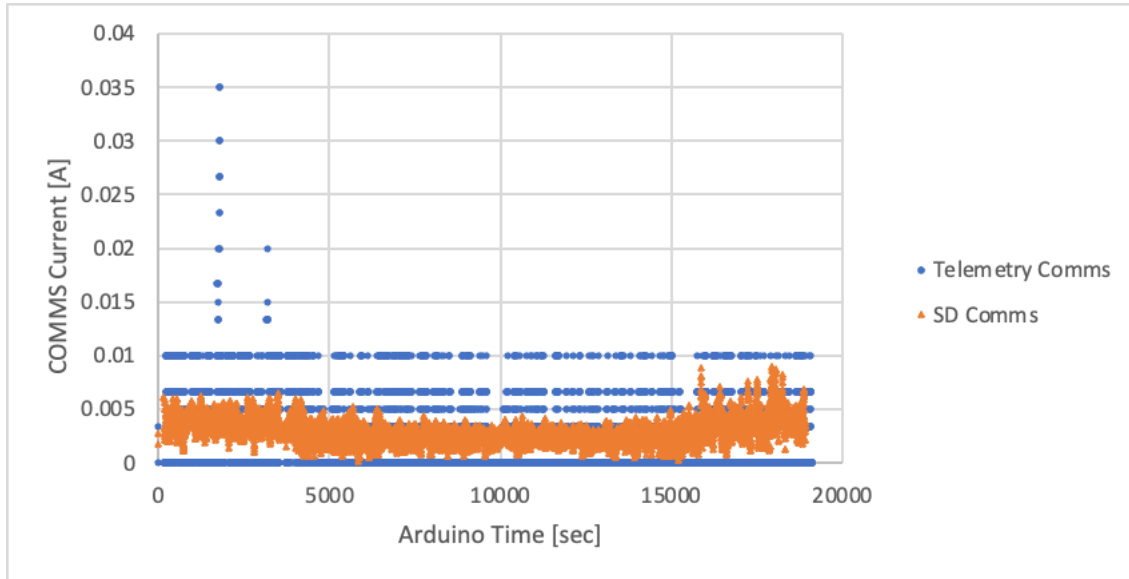


Figure 33: Comparison of SD COMMS current data to the downlink telemetry COMMS current data.

Figure 34 illustrates the current pulled from the TMS throughout the flight. Current appears to remain steady and within the predicted range of 0 to 0.1 amps. There is a spike in current around 150 seconds, before the flight occurred.

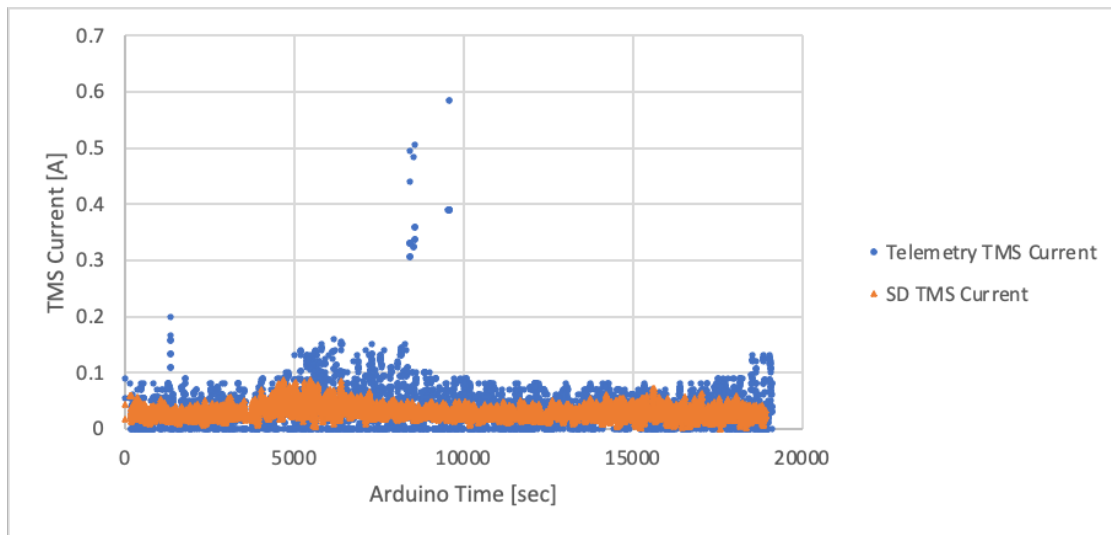


Figure 34: Comparison of SD TMS current data to downlink telemetry TMS current data

The Geiger Counters had a default setting to “toggle”. When the Geiger Counters were toggling, we expected there to be fluctuating current from high to low while the Geiger counters were turning on and off. Figure 35 demonstrates the fluctuating current draw which can be seen in the

jagged appearance of the data spread. There was a drastic increase of current after 5000 seconds from the turn-on time. The data taken from the SD matches the telemetry data very closely. This shows a likely time scale variation between the internal Arduino clock and that from the telemetry. The observed increase in current might be when the radiation doors jammed, but there is no other evidence of this.

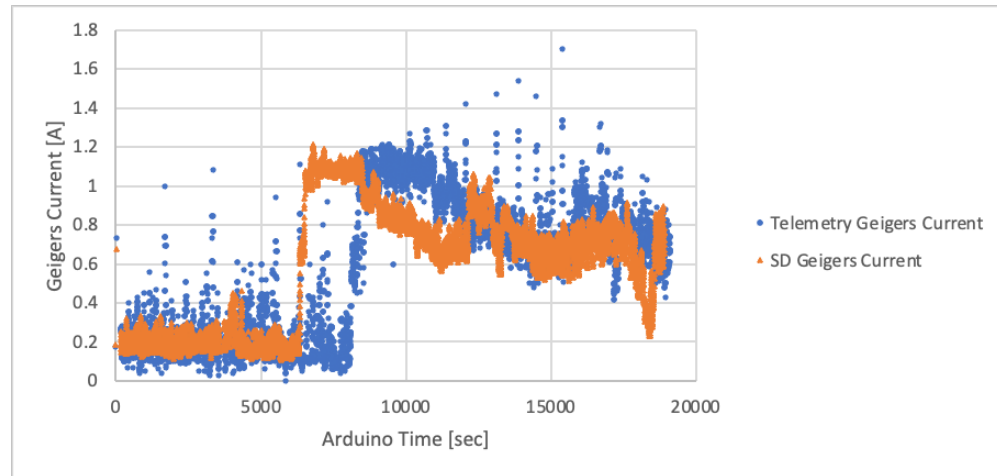


Figure 35: Comparison of SD Geiger's current data to the downlink telemetry current data.

Figure 36 displays the current pulled from the GPS system, Altimeter, and the 9Dof stick. We expected extremely low current, and the graph displays a current of about 0.025 amps. In this case the SD data matched the telemetry data almost perfectly however there was a noticeable trend where it looked like the telemetry data lagged behind the SD card data. This may have been caused by a different time scale between the two clocks. The telemetry data set has a few outliers, but most of these appear to happen before flight. Throughout the flight the GPS had the most constant and unshifting current draw out of all the subsystems.

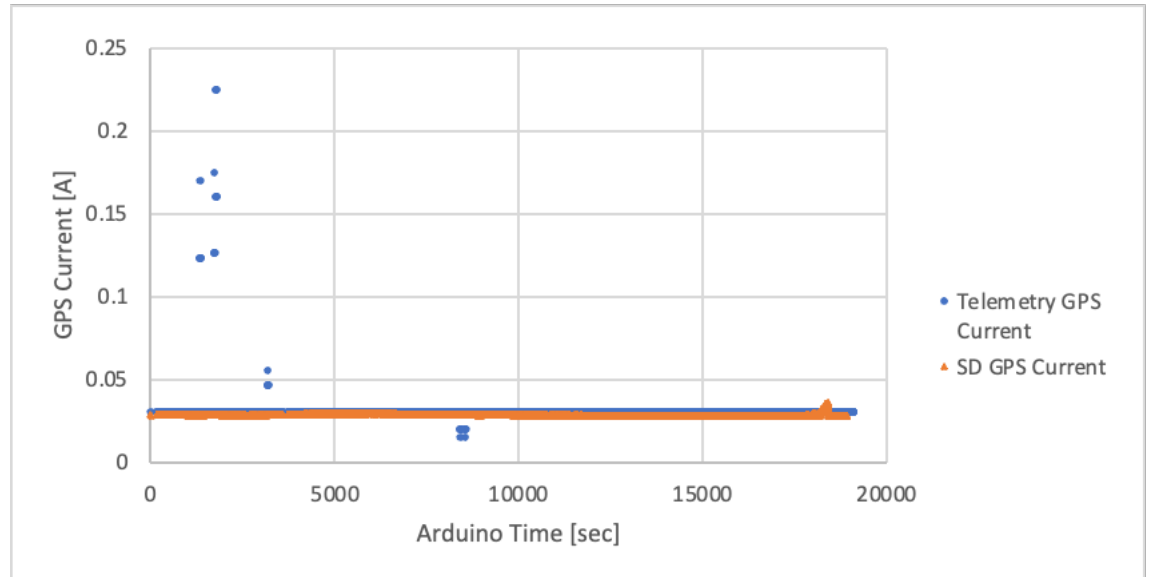


Figure 36: Comparison of SD current data for the GPS and altimeter to the downlink telemetry current data.

The Mobius Camera's current draw pre-flight and during flight is shown in Figure 37. The current appears to repeatedly spike before 5000 seconds. The mobius camera had a default setting to be toggling similar to the Geiger's. After reviewing the footage, it does not seem like the Mobius camera was toggling correctly. This could be why the current during the flight looks like a giant mass of random data points. We did expect the Mobius camera to have a relatively higher current draw, which is reflected in the graph with a range of 0 to 0.5 amps. The current data for the mobius camera is difficult to dissect, but it does appear to show that the camera was pulling current for most of the flight. The telemetry data appears to have more gaps in between data points than the SD data. The SD data also does not reach some of the higher amperages that the telemetry data reaches. The toggle duration was ten seconds, and the telemetry interval was about 15 seconds. This time difference caused more gaps in the telemetry data.

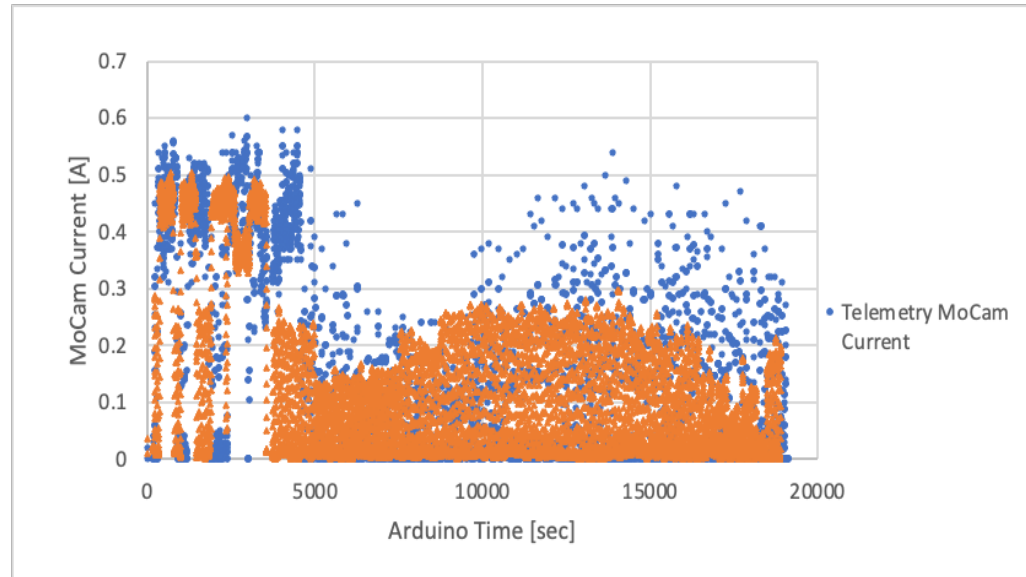


Figure 37: Comparison of SD current data for the Mobius camera to the downlink telemetry current data.

Analyzing Figure 35 showed a dramatic increase in current after 8,000 seconds Arduino time. Figure 38 illustrates a closer view of this occurrence. There are a few possibilities that could have caused the current to increase. At some point during the flight the door on the housing for the Geiger's got jammed, this could cause the current to spike like it is in Figure 39. We cannot definitively say this is the case because we are not sure at what time the door jammed, but it is a possibility.

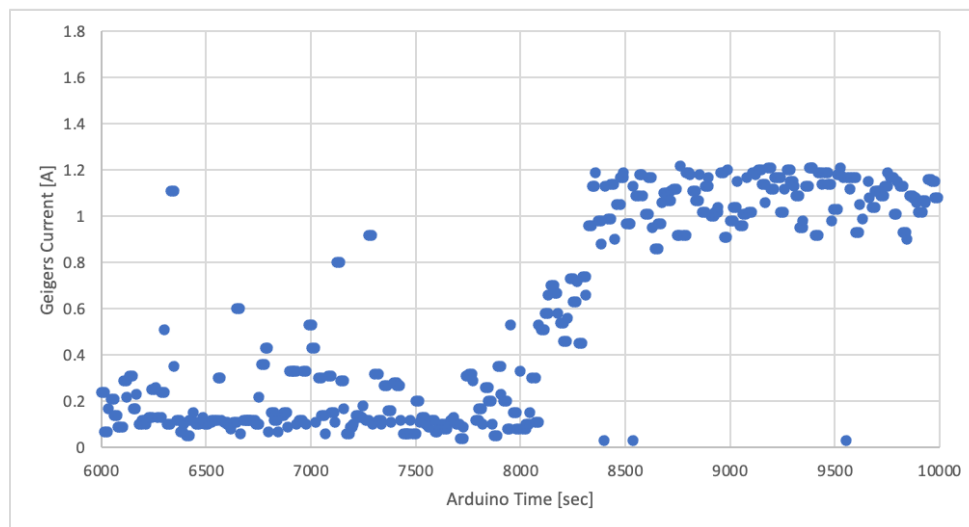


Figure 38: Close up view at the beginning of flight, of current draw from Geiger Counters and the servo.

Figure 39 demonstrates spiky current draw before 5,000 seconds from the mobius camera. Majority of the current data in Figure 39 was collected before flight. For testing purposes before the flight, commands were sent to the mobius camera to ensure telemetry downlink was operating and communication to the HASP team worked. The Mobius camera was designed to toggle which is represented in Figure 39 below.

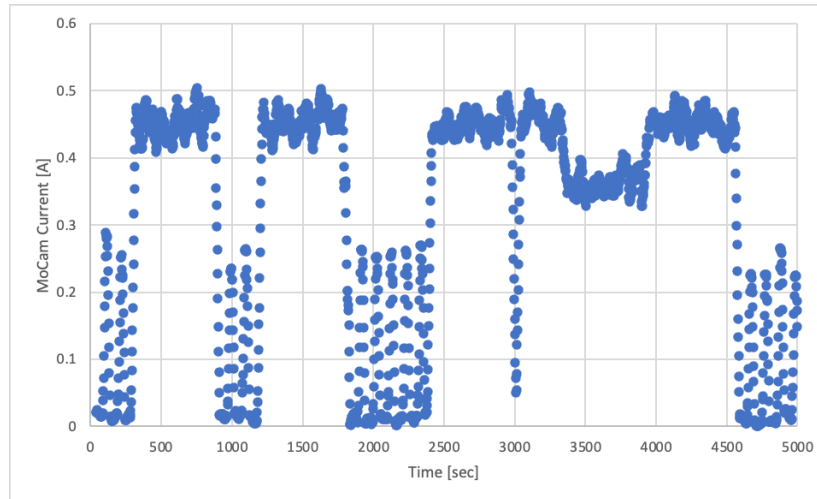


Figure 39: Close up view of the Mobius Camera current draw before the flight.

Towards the end of flight, around 19:56 UTC our payload failed. Commands were no longer being received and we noticed no current was being pulled. After looking at the current draw from the PMS there doesn't seem to be an irregularity towards the end of our data recording. A more isolated examination of the COMMS current draw towards the end of flight shows some slight change in current draw. The current starts reaching more "extreme" peaks after 20,000 seconds as shown in Figure 40. Although the peaks are higher than before they are still relatively low reaching a max of .009 amps.

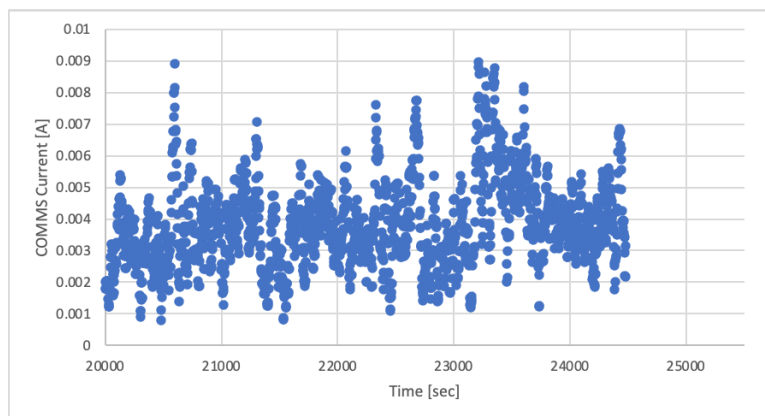


Figure 40: The COMMS current draw at the end of flight, demonstrating increases in current.

In conclusion, the SD data matched the telemetry data relatively well. Certain subsystems appeared to have outliers, but after closer examinations the current draw was not unusual and did not differ far from the expected current draw. Analyzing current towards the end of flight does not provide a conclusive answer to why the payload failed and current draw dropped to less than 0.01 amps.

6.4. GPS and 9DOF

GPS data was used to determine the altitude and coordinates of the payload. The altitude of the Payload over the HASP flight can be seen in Figure 41.

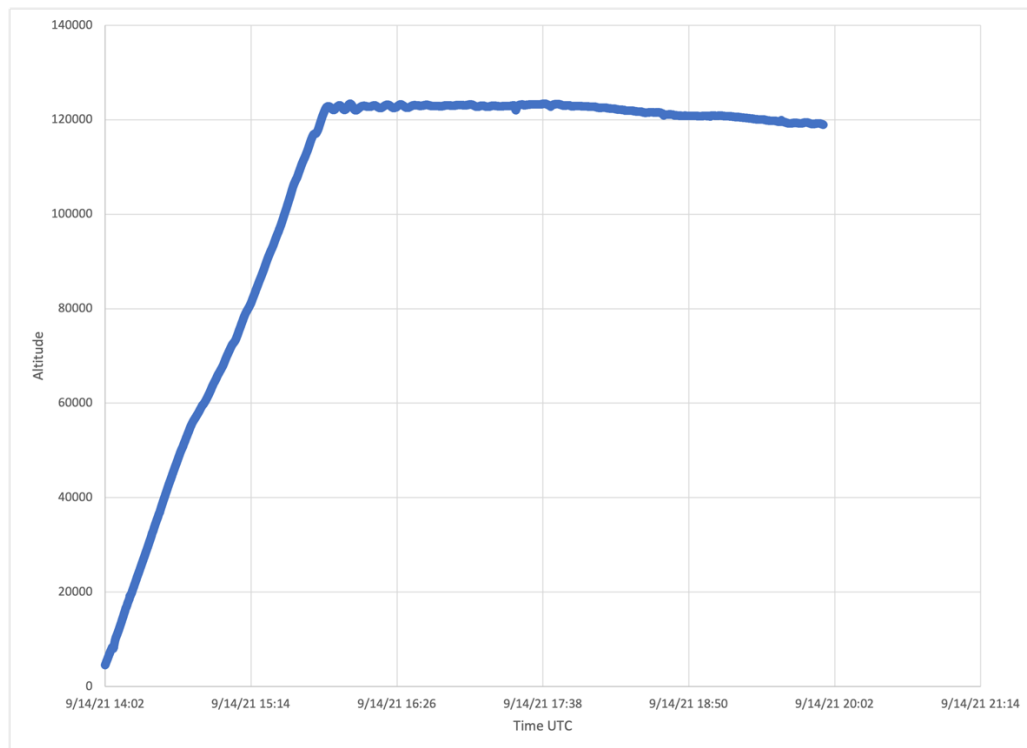


Figure 41: Payload Altitude over Time from Altus Metrum TeleGPS

The payload reached a maximum altitude of 123,390 ft. GPS power was lost at 19:56 UTC. The payload coordinates recorded from the GPS were used to find the sun angle from vertical seen in Figure 42.

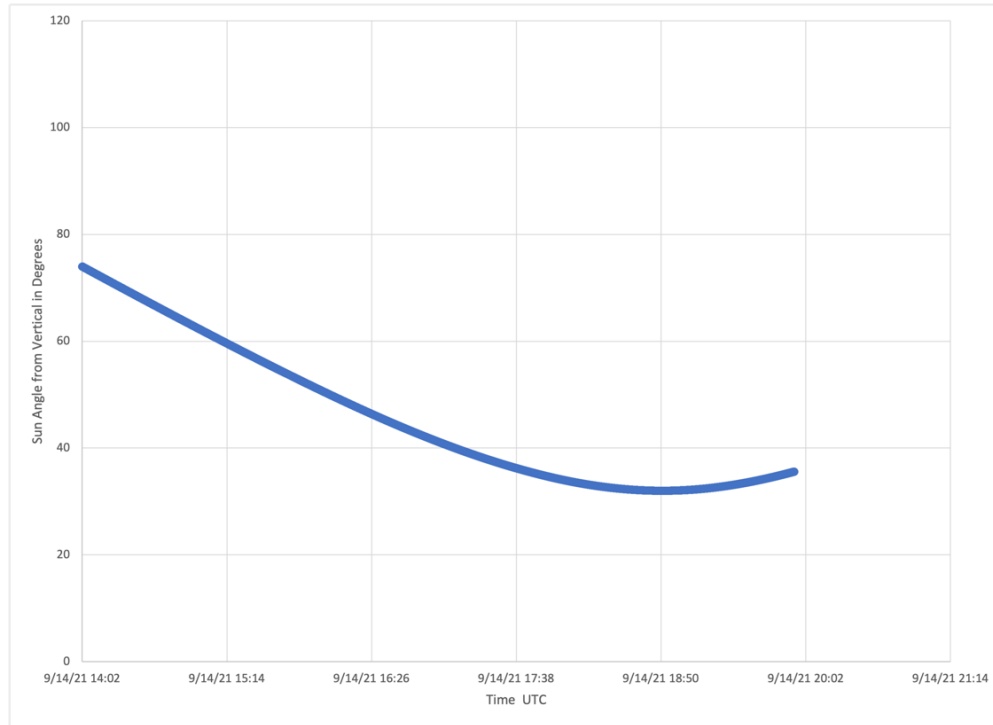


Figure 42: Sun Angle from Vertical vs. Time

The Sun angle relative to the payload location decreased over the launch as expected. The magnetometer was used to determine the rotation of the payload over the flight. The payload fluctuated 1.8 degrees from vertical z-axis according to the accelerometer data. The rotation of the payload throughout the flight can be seen in Figure 43.

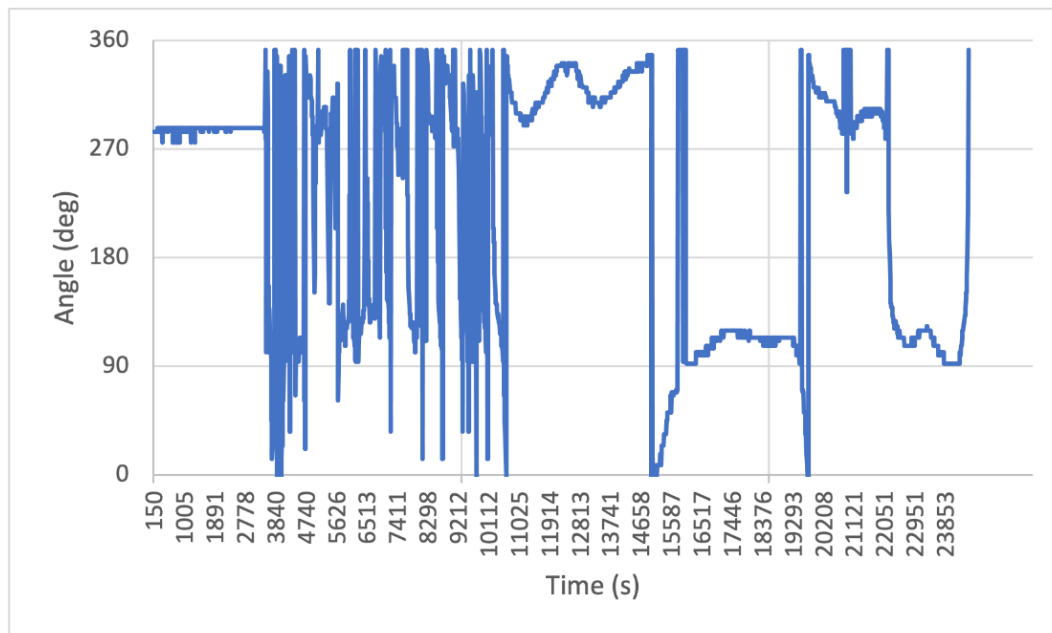


Figure 43: Azimuth Angle of Payload Orientation versus Time

The data were adjusted towards true north using the magnetic declination for Fort Sumner where the payload was launched.

7.0 Failure Summary

The payload performed well, receiving commands and relaying adequate data to the team. However, the current became low in the middle of the day and did not return. The TMS was unable to identify if it was high temperature that damaged the payload. The largest failure was that the Geiger enclosure door jammed in the open position. The data suggests that the door was jammed before the flight took place from when it was shipped to when power was received. The onboard camera saved incomplete files and did not record proper time stamps. After other on-hand Mobius cameras were found to be faulty, a different camera system should be considered for future flights. The rechargeable lithium ion battery chosen to fit the flight specification but seemed to be unreliable, possibly because of previous damage. Several of these batteries were unable to hold a charge after being used in testing our team is not confident in their reliability.

8.0 Conclusions

The radiation versus altitude and time experiment found no distinguishable difference in CPM when the brass shutter was opened and shut. During post assessment the brass door was found to be jammed in the open position. It is unknown when this anomaly occurred and most likely explains why we were not able to see a significant difference in the CPM when the door was open and when it was closed. This means we were unable to differentiate gamma from alpha and beta ionizing radiation. The red Geiger-Muller detectors recorded fewer counts than the pocket solid-state detectors as altitude increased, but more counts during the float. With the shutter working there may have been an indication of what type of radiation the Geiger-Muller does and does not detect. The bottom-facing detectors recorded increased counts in the middle of the payload's ascent, possibly due to atmospheric back-scattering of ionizing radiation. The bottom-facing detectors recorded very few counts during float and no dependence on sun angle was observed. The counts were highest for both types of detectors at the minimal sun angle of 35 degrees and decreased significantly as the sun angle increased to 45 degrees. Of these data the red Geiger-Muller detectors recorded higher counts than the Pocket Geiger counters. The data from the Geiger counters was difficult to interpret because there were multiple small files and one large file on the SD card. From the Arduino time stamp the data was lined up to launch. The file did not match the flight length until power was lost, but some of the Arduinos have been known to have inconsistent internal clocks. The payload lost power around mid-day suggesting that the payload may have overheated. However, there isn't a sudden increase in temperature recorded from the TMS. The temperature sensor next to the camera was the only one that recorded a temperature hotter than expected. The power was investigated and found that there wasn't any large increase that would have blown the fuse on the HASP side. The camera only

recorded a few segments through-out the flight suggesting that the on-board battery was dead. The COMMS system worked, with uplink and downlink working as expected throughout the flight.

The team created a poster that was presented at the Fort Lewis College Physics & Engineering Fall welcome event. This was one of approximately 30 group presentations about their summer projects. Unfortunately, the flight had not happened at the time of this event. The team is planning on updating the poster for presentation at the end-of-the-year Natural and Behavioral Sciences symposium.



Figure 44: Poster presentation at the Fort Lewis College Physics & Engineering Fall Welcome

Radiation vs. Altitude and Time (RAT) Payload for the High Altitude Student Platform (HASP)

Hannah Carlson, Jessie Urban, Daniel Sandner, Humberto Arredondo Perez, Roxie Sandoval, Nikolas Conny, Cheyenne Tucson
Faculty Advisor: Dr. Charles Hakes
Fort Lewis College Department of Physics and Engineering
1000 Rim Dr, Durango, CO 81301

Abstract

The goal of the project was to design and construct a payload to monitor atmospheric radiation on the High-Altitude Student Platform (HASP). The payload will fly to an altitude of about 22 miles by a zero-pressure balloon. Most of the systems have uplink command capabilities and are able to download data as well as store data locally. The payload is set to launch mid-September 2021 from Fort Sumner NASA balloon facility.

Structure

The completed payload structure consists of a sled that slides within an outer shell made of G10 fiberglass. One side houses all the main payload electrical systems and the other side holds the Geiger counters for the radiation experiment.

Figure 1. Payload structure, the outer case on the left and the sled on the right.

Radiation Experiment

The RAT Payload was to collect radiation data on board a NASA weather balloon. To do so, we implemented two types of Geiger counters – solid state and Geiger muller tube Geiger counters. The Geiger counters were enclosed within a brass Faraday Cage with mechanical, opening doors. Over the course of the flight, the doors opened and closed on a determined time interval, allowing the Geiger counters to count Alpha particles when the doors were open, and Beta and Gamma particles when the doors were closed. All data was transmitted off HASP via the COMMS system as well as uploaded to an SD card.

Figure 4. The Geiger system, which includes the SD card, servo and the Arduino.

Communications System (Comms)

The COMMS system communicates between all subsystems through Inter-integrated circuit (I2C). I2C is a serial communication bus that uses two wires: SDA and SCL. Data is transferred bit by bit along the SDA line.

Figure 2. I2C communication between two devices.

Figure 11. Hannah working on COMMS.

Power Management System (PMS)

The PMS Provides power to each sub-system on the payload and monitors it using DC Current sensors. This is used to trouble shoot a potential failure.

Figure 3. PMS Mounted in HASP payload.

Thermal Management System (TMS)

Each temperature sensor records the surrounding temperature around the Arduino board of each subsystem, so if they reach a temperature less than -20 degrees Fahrenheit, then the heaters turn on to keep the systems from freezing and stop working. The data is saved to an SD card as well as written to the communication system.

Figure 6. The resistor (left) used as a heater and the temperature sensor (right) used in the TMS system.

Mobius® Camera Board

An on-board Mobius camera was used to verify the sun's location. The camera was controlled by an Arduino with three uplink commands. Toggle was used the most during flight which is 19s on 81s off. During takeoff and landing the camera was set to on. The camera off command was used to lower the payload's current.

Figure 8. Mobius camera mounted in payload.

Command	Hex Value	Function
*BP	42.30	Turn MacCam off
*B1	42.31	Turn MacCam on
*B2	42.32	Set MacCam to loggie
*CP	43.30	Turn heater's setpoint to -20°F
*C1	43.31	Turn heater's setpoint to 40°C
*EP	45.30	Turn heaters off
*E1	45.31	Turn heaters on
*FP	46.30	Turn Geigers off
*F1	46.31	Turn Geigers on with doors closed
*F2	46.32	Turn Geigers on with doors open
*F3	46.33	Set Geigers to loggie

Figure 45: FLC HASP Team poster at Physics & Engineering Fall Welcome Event

9.0 Message to Next Year

This year our team performed a successful HASP flight. During the flight, a mechanical error occurred causing the brass shutter to get stuck in the open position. The system in the future should have more protection from outside contact. The system lost power towards the end of the flight, after a post-flight assessment the cause is still unknown. A different camera system should be considered for future flights because of multiple copies of the cameras being found faulty. The battery chosen to fit the flight specification but seemed to be unreliable. A different, or newer battery should be used that has a greater depth of charge. Future teams should include multiple engineers proficient in programming as that was the part of the project we struggled with the most. This project is a great introduction to aerospace and teaches the design and engineering process used in satellites fabrication. There were a few part-time members working on this project this summer. More full-time members would reduce last minute work.



Figure 46: Team photo at Columbia Scientific Balloon Facility

References

- [1] “Geiger counter (old-school),” *SEN-09298 - SparkFun Electronics*. [Online]. Available: <https://www.sparkfun.com/products/retired/9298>. [Accessed: 02-Dec-2021].
- [2] “Infographic: How a geiger counter works,” *Inside Science*. [Online]. Available: <https://www.insidescience.org/news/infographic-how-geiger-counter-works>. [Accessed: 02-Dec-2021].
- [4] C. W. Fabjan, “Solid State Detectors,” *Solid State Detectors - an overview | ScienceDirect Topics*, 2003. [Online]. Available: <https://www.sciencedirect.com/topics/mathematics/solid-state-detectors>. [Accessed: 09-Jan-2021].
- [5] “Solid-state detector,” *Encyclopædia Britannica*, 07-Feb-2011. [Online]. Available: <https://www.britannica.com/science/solid-state-detector>. [Accessed: 09-Jan-2021].
- [6] “How to Setup I2C Communication on the Arduino,” *Circuit Basics*, 16-Nov-2021. [Online]. Available: <https://www.circuitbasics.com/how-to-set-up-i2c-communication-for-arduino/>. [Accessed: 05-Dec-2021].